

Global and Tail Dependence: A Differential Geometry Approach

Davide Lauria* Svetlozar T. Rachev[†]

A. Alexandre Trindade[‡]

June 11, 2021

Abstract

Measures of tail dependence between random variables aim to numerically quantify the degree of association between their extreme realizations. Existing tail dependence coefficients (TDCs) are based on an asymptotic analysis of relevant conditional probabilities, and do not provide a complete framework in which to compare extreme dependence between two random variables. In fact, for many important classes of bivariate distributions, these coefficients take on non-informative boundary values. We propose a new approach by first considering global measures based on the surface area of the conditional cumulative probability in copula space, normalized with respect to departures from independence and scaled by the difference between the two boundary copulas of co-monotonicity and counter-monotonicity. The measures could be approached by cumulating probability on either the lower left or upper right domain of the copula space, and offer the novel perspective of being able to differentiate asymmetric dependence with respect to direction of conditioning. The resulting TDCs produce a smoother and more refined taxonomy of tail dependence. The empirical performance of the measures is examined in a simulated data context, and illustrated through a case study examining tail dependence between stock indices.

Introduction

The analysis of the extremal dependence between two random variables takes on great importance in a wide range of scientific disciplines and applications like computer science, environmental engineering, meteorology, risk management, and finance. *Tail dependence coefficients* (TDCs) between two random variables X and Y , with joint distribution function H and marginal distribution functions F and G respectively, were introduced by [44] in order to measure the

*Texas Tech University, Department of Mathematics & Statistics, Lubbock TX 79409-1042, U.S.A., Davide.Lauria@ttu.edu

[†]Texas Tech University, Department of Mathematics & Statistics, Lubbock TX 79409-1042, U.S.A., Zari.Rachev@ttu.edu

[‡]Texas Tech University, Department of Mathematics & Statistics, Lubbock TX 79409-1042, U.S.A., Alex.Trindade@ttu.edu.

dependence between their extreme realizations. The lower TDC is a measure of the dependence in the lower-left quadrant and is defined as:

$$\lambda_l(X|Y) = \lim_{\alpha \rightarrow 0^+} \mathbb{P}[X \leq F^{-1}(\alpha) | Y \leq G^{-1}(\alpha)] = \lim_{\alpha \rightarrow 0^+} \frac{C(u, v)}{v}. \quad (1)$$

Analogously, the upper TDC measures dependence in the upper-right quadrant as:

$$\lambda_u(X|Y) = \lim_{\alpha \rightarrow 1^-} \mathbb{P}[X > F^{-1}(\alpha) | Y > G^{-1}(\alpha)] = \lim_{\alpha \rightarrow 1^-} \frac{1 - u - v + C(u, v)}{1 - v}. \quad (2)$$

Note that Sklar's theorem (Theorem A.2 in Appendix A) immediately implies that λ_l and λ_u are completely determined by the implied copula C that connects H , F , and G . Both measures are confined to the interval $[0, 1]$, where a zero value denotes tail independence¹.

TDCs, also known as *strong* TDCs, are intuitively simple to understand, but suffer from important theoretical and practical drawbacks. In particular, two main limitations have been pointed out: (i) the coefficients do not convey any information on the rate of convergence of the limit in (1)–(2), and (ii) the dependence is measured only along the diagonal $x = y$. The consequence, from a practical perspective, is that TDCs assume their boundary values, zero or one, for many popular distribution classes, leading to a weak taxonomy of the behavior of the conditional structure for joint extreme events.

The case of elliptically contoured distributions provides an illustrative example. An n -dimensional random vector Z is called elliptically distributed with parameters $\mu \in \mathbb{R}^n$ and $\Sigma \in \mathbb{R}^{n \times n}$ if $Z \stackrel{d}{=} \mu + R_n A' U$, where $A \in \mathbb{R}^{n \times n}$, with $A'A = \Sigma$ and $\text{rank}(\Sigma) = n$. R_n is a random variable with distribution F_n , called the generating distribution, and U is an n -dimensional random vector uniformly distributed on the unit sphere, and independent of R_n . The random variable $E \stackrel{d}{=} R_n U$ is then called spherically distributed, and each margin of Z has the same distribution G . Schmidt [41] proved that if F_n has a regularly varying tail, then all bivariate margins of Z are tail dependent (the TDCs are strictly positive); furthermore, the TDCs of any bivariate marginal extracted from an elliptically contoured distribution are greater than zero if the survival function \bar{G} of the random variable Y is O -regularly varying; if G has instead a regularly varying tail, then all bivariate margins have tail dependence. Multivariate normal, logistic, and symmetric generalized hyperbolic distributions, for instance, are elliptical distributions with bivariate margins which are tail independent. A multivariate t -distribution with ν degree of freedom and linear correlation coefficient ρ , has instead positive TDCs given by

$$\lambda_l = \lambda_u = 2t_{\nu+1} \left(-\sqrt{\left(\frac{(\nu+1)(1-\rho)}{1+\rho} \right)} \right). \quad (3)$$

where $t_\nu(x)$ is the density function of the univariate t with ν degrees of freedom.

Another important example is given by the class of multivariate *generalized hyperbolic* (GH) distributions introduced in [2]. GH distributions play an important role in financial modeling, in particular for their flexibility in capturing

¹They have been generalized to random vectors of dimensions greater than two; see [27] for a review.

particular stylized facts like asymmetries and fatter tails with respect to the Gaussian case [1, 3, 11, 4, 23, 45]. Hammerstein, [19, Theorem 4], showed that TDCs for bivariate margins extracted from multivariate GH distributions can only assume the values of zero or one; the only exception being the multivariate scaled and shifted t -distribution (which has equal lower and upper coefficients). A brief summary of bivariate GH distributions can be found in Appendix C.

Again, as for elliptical distributions, this result is in contrast to the evidence that dependence structures in the lower-left and upper-right quadrants can be substantially greater than the independent case, and also for parameter settings that produce TDCs equal to zero. Furthermore, these extreme dependence relationships can assume a wide range of behaviours. Consequently, classification of tail dependence for these kinds of distributions is poor, and with limited practical application. Indeed, even in the bivariate Gaussian case when both marginals have light-tails, it is evident that the degree of tail dependence in the west-lower (east-upper) corner of the support changes considerably as the correlation coefficient increases toward one.

The first attempt at improving TDCs measured the speed at which the conditional probability varies in the joint tails. [28] based their analysis on the idea that the joint distribution H is in the domain of attraction of some multivariate extreme value distribution. Restricting attention to the two-dimensional case of interest in our paper, they first considered transformations

$$Z_1 = \frac{-1}{\log F(X)} \quad \text{and} \quad Z_2 = \frac{-1}{\log G(Y)}, \quad (4)$$

so that the joint distribution H_Z of $[Z_1, Z_2]$ satisfies $H_Z(z_1, z_2) = H(x, y)$, where Z_1 and Z_2 follow a Fréchet distribution, i.e., $P(Z_i \leq z) = e^{-1/z}$, for $i = 1, 2$. The behaviour of the joint distribution is then modelled by assuming the following asymptotic result

$$P(Z_1 > z, Z_2 > z) \sim \ell(z)z^{-\frac{1}{\eta}}, \quad z \rightarrow \infty, \quad (5)$$

where $\ell(z)$ is a slowly varying function and $1/2 \leq \eta \leq 1$. It can be shown that if $\eta = 1$ and $\lim_{z \rightarrow \infty} \ell(z) = \lambda > 0$, then X and Y are upper tail dependent with $\lambda_u = \lambda$. If instead $\lim_{z \rightarrow \infty} \ell(z) = 0$, then $\lambda_u = 0$ and $\eta < 1$. In other words, if $\ell(z)$ converges to zero, we do not have asymptotic dependence since the upper TDC is equal to zero. (The value of η can be interpreted as the rate at which the dependence decreases in the joint upper tail ².)

A strictly connected measure is the *weak* coefficient of tail dependence χ , defined by [9] as

$$\chi_l = \lim_{\alpha \rightarrow 0^+} \frac{\log [P(U \leq \alpha)P(V \leq \alpha)]}{\log [P(U \leq \alpha, V \leq \alpha)]} - 1 = \lim_{\alpha \rightarrow 0^+} \frac{2 \log \alpha}{\log [C(\alpha, \alpha)]} - 1, \quad (6)$$

for the lower tail, and

$$\chi_u = \lim_{\alpha \rightarrow 1^-} \frac{\log [P(U > \alpha)P(V > \alpha)]}{\log [P(U > \alpha, V > \alpha)]} - 1 = \lim_{\alpha \rightarrow 1^-} \frac{2 \log (1 - \alpha)}{\log [1 - 2\alpha + C(\alpha, \alpha)]} - 1, \quad (7)$$

for the upper tail, where $U = F^{-1}(X)$ and $V = G^{-1}(Y)$. Curiously, the coefficient η in (5) is related to χ through the equation $\chi = 2\eta - 1$, meaning

²The idea was then further developed in [25], where concepts of tail order (the ratio $\frac{1}{\eta}$) and tail order function have been introduced, see also paragraph 2.16 in [27].

that computation of the two coefficients are one and the same. This property has been exploited in order to compute χ for particular classes of multivariate distributions. [40] for instance, obtain that $\chi_l = \chi_u = \sqrt{2(1+\rho)} - 1$ for the class of elliptical GH distributions with $\rho \geq 0$, where ρ is the correlation coefficient between X and Y , whereas in the Gaussian special case we have instead $\chi_l = \chi_u = \rho$. The result is encouraging since it means χ contains information on the rate at which the conditional probability changes as we move either southwest (lower) or northeast (upper) on the support. It is therefore able to detect positive tail dependence also in the case of semi-heavy marginal tails, offering the possibility of potential improvements with respect to TDCs. ([20] compute the values of χ for various well known copulas.)

At this point we have two measures of tail dependence: the weak (χ) and the strong (λ). The former is applicable in detecting “weak” tail dependence structures (meaning that they disappear asymptotically); the latter is instead better suited for assessing asymptotic tail dependence. A potential drawback, as pointed out by [17], among others, is that all these measures compute tail dependence by focusing only on the main diagonal $u = v$ of the copula support. The implications of this are possible under-estimation of the joint tail risk [16]. In order to avoid this limitation, [17] proposed reformulating weak TDCs by moving along the path of maximal tail dependence. That is, both weak and strong TDCs should be computed along the path where the copula assumes its largest values on its way toward $(0, 0)$ (for lower tail dependence), and toward $(1, 1)$ (for upper tail dependence).

In empirical finance, both strong and weak TDCs are often computed via nonparametric methods based on extreme value theory. An example is the estimator proposed by [22], which is directly applied to (5) in order to estimate η . Other nonparametric estimators of tail dependence can be found in [42], [39], and [13]. These methods have the advantage of avoiding the aforementioned limitation in the TDCs, since they do not rely on direct computation of the limits with respect to a particular copula. However, nonparametric approaches usually rely on the specification of tuning parameters (in these cases threshold constants that determine the extreme region), leading to suboptimal solutions attained by means of intensive optimization routines.

Dependence in extreme values of random variables is assuming a central role in risk management, and financial and insurance processes offer, in this regard, an important source of examples. The high level of integration in modern economies, the progress of information technology, and the growing number of agents at play in financial markets, are just some of the factors that seem to have contributed to increased dependence in the extremes of financial variables, as a growing number of empirical studies are showing. [37], [29], and [5] studied extreme correlation in international equity markets. [36] investigated the dependence in both extreme losses and extreme gains between the S&P 500 index and the various indices representing specific countries’ stock markets, finding that the former type of dependence is greater than the latter. [21] use the analysis of extremal dependency between the S&P 500 index and VIX futures contracts in order to better hedge the risk of a long portfolio on the index. In some cases dependence among extremes seems to be determined by the structure of the phenomenon itself, as occurs for example between the daily volatility of financial returns and the number of transactions [38]; or between extremes in returns and trading volumes in Asian stock markets [35]. In risk management,

tail dependence is also strongly connected with the concept of risk dependence [6, 12, 21].

In this work we propose new TDCs to quantify the degree of lower and upper tail dependence between two random variables. The idea stems from global dependence measures defined through surface integrals of the copula function, suitably normalized with respect to the independence case, and scaled by the difference between the Fréchet-Hoeffding upper and lower bounds. These global measures are developed in Section 1. The proposed TDCs, introduced in Section 2, do not rely on particular paths chosen in the copula domain, nor on predefined regions of the support. They are able to detect positive dependence structures in terms of joint probabilities greater than the independence case, and in the joint tails for any asymptotic behaviour of the associated marginals. They can also provide information on the strength of tail dependence, both in the case of asymptotic dependence, as well as in the case of asymptotic independence.

The rest of the paper is organized as follows. A simulation study is conducted in Section 3 in order to assess the performance of maximum likelihood estimation in parametric modeling of the proposed TDCs, while Section 4 undertakes a case study to illustrate their usage in an empirical financial setting investigating tail dependence structures between some very visible stock indices. The development of the global measures in Section 1 requires familiarity with fundamental concepts and results from copula theory and associated measures of dependence and of concordance, and thus these are distilled into a summary in Appendix A. Proofs of more difficult theorems are relegated to Appendix B, while a description of several copulas used throughout the paper is provided in Appendix C.

1 Global Dependence

Our proposed measure of tail dependence begins with a global formulation aimed at the entire distribution, in analogy with other global measures such as the correlation coefficient, Kendall's tau, and Spearman's rho. Let $C(u, v)$ be the unique bivariate copula associated with the joint distribution function $H(x, y)$ of the continuous bivariate random vector (X, Y) , whose marginal cumulative distribution functions are $F(x)$ and $G(y)$, respectively. The material in this section assumes familiarity with basic copula theory and associated measures of dependence, a summary of which is provided in Appendix A. Also, proofs of theorems not given or alluded to in the text may be found in Appendix B.

Definition 1.1. For the subsets of the unit square in \mathbb{R}^2

$$D_v = \{(u, v) : u \in [0, 1], v \in (0, 1]\}, \quad \text{and} \quad D_u = \{(u, v) : u \in (0, 1], v \in [0, 1]\},$$

let the functions $\Psi_{X|Y}^{(l)} : D_v \rightarrow [0, 1]$ and $\Psi_{Y|X}^{(l)} : D_u \rightarrow [0, 1]$ be defined as

$$\Psi_{X|Y}^{(l)}(u, v) := \frac{C(u, v)}{v}, \quad \text{and} \quad \Psi_{Y|X}^{(l)}(u, v) := \frac{C(u, v)}{u}, \quad (8)$$

which represent the *lower* cumulative conditional probabilities $P(X \leq x|Y \leq y)$ and $P(Y \leq y|X \leq x)$, respectively.

One way to describe the functions in (8) is that they represent conditionals in the direction of the SW portion of the unit square (hence *lower*). Based on the Fréchet-Hoeffding bounds W and M on any given copula C (see Theorem A.4), we can apply the same idea to define the conditional Fréchet-Hoeffding boundary functions

$$\mathbb{W}_{X|Y} = \frac{W(u, v)}{v}, \quad \mathbb{W}_{Y|X} = \frac{W(u, v)}{u}, \quad \mathbb{M}_{X|Y} = \frac{M(u, v)}{v}, \quad \mathbb{M}_{Y|X} = \frac{M(u, v)}{u}. \quad (9)$$

Not surprisingly, the unconditional Fréchet-Hoeffding bounds also apply in this conditional probability framework.

Theorem 1.1. For every copula $C(u, v)$ and every (u, v) in $[0, 1] \times (0, 1]$, we have

$$\mathbb{W}_{X|Y}(u, v) \leq \Psi_{X|Y}^{(l)}(u, v) \leq \mathbb{M}_{X|Y}(u, v), \quad (10)$$

and

$$\mathbb{W}_{Y|X}(u, v) \leq \Psi_{Y|X}^{(l)}(u, v) \leq \mathbb{M}_{Y|X}(u, v). \quad (11)$$

Proof. Consider $\Psi_{X|Y}^{(l)}$, then, given that v can take values in $(0, 1]$ and that copula functions are non-decreasing in each argument, the two inequalities follow directly from Fréchet-Hoeffding bounds. Similar reasoning applies to $\Psi_{Y|X}^{(l)}$. \square

Note that if C is a symmetric copula, then $\Psi_{X|Y}^{(l)}$ and $\Psi_{Y|X}^{(l)}$ are symmetric about the line $v = u$. We now consider some properties of the functions $\Psi_{X|Y}^{(l)}(u, v)$. Similar results follow straightforwardly for $\Psi_{Y|X}^{(l)}(u, v)$. We start by studying the behaviour of function $\Psi_{X|Y}^{(l)}$ on the boundary of its domain: $\Psi_{X|Y}^{(l)}(u, 1) = C(u, 1) = u$, $\Psi_{X|Y}^{(l)}(1, v) = C(1, v) = v/v = 1$, and $\Psi_{X|Y}^{(l)}(0, v) = 0/v = 0$. Now, $\Psi_{X|Y}^{(l)}(u, v)$ is not defined when $v = 0$, but we can study the limit $\lim_{v \rightarrow 0} \Psi_{X|Y}^{(l)}(u_0, v)$ for some choice of $u_0 \in [0, 1]$. Consider for instance the functions $\mathbb{W}_{X|Y}$ and $\mathbb{M}_{X|Y}$. We can compute for any $u_0 \in [0, 1]$

$$\lim_{v \rightarrow 0} \mathbb{W}_{X|Y}(u_0, v) = \lim_{v \rightarrow 0} \frac{1}{2v} (|u_0 + v - 1| + u_0 + v - 1) = 0, \quad (12)$$

$$\lim_{v \rightarrow 0} \mathbb{M}_{X|Y}(u_0, v) = \lim_{v \rightarrow 0} \frac{1}{2v} (u_0 + v - |u_0 - v|) = 1. \quad (13)$$

Now, given the above limits and the two inequalities in (10), we can state that

$$0 \leq \lim_{v \rightarrow 0} \Psi_{X|Y}^{(l)}(u_0, v) \leq 1, \quad \text{for all } u_0 \in [0, 1]. \quad (14)$$

In other words, the boundary $\partial\Omega$ of a surface like $\Psi_{X|Y}^{(l)}$ can be divided into two parts: $\partial\Omega_1$ and $\partial\Omega_2$. The first part is common to any surface and can be defined as $\partial\Omega_1 = D_1 \cup D_2 \cup D_3$, where $D_1 = \{(u, v, z) : u = 0, v \in [0, 1], z = 0\}$, $D_2 = \{(u, v, z) : u \in [0, 1], v = 1, z = u\}$, and $D_3 = \{(u, v, z) : u = 1, v \in [0, 1], z = 1\}$. The second part will depend instead on the particular copula C under consideration, and it is bounded between $\{(u, v, z) : u \in [0, 1], v = 0, z = 0\}$ and $\{(u, v, z) : u \in [0, 1], v = 1, z = 0\}$. Noting Theorem A.1, we can also state that

$\partial\Omega_2$ will be a non-decreasing curve from point $(0,0,0)$ to point $(1,0,1)$. Since the Ψ functions are, in general, not grounded, they are also not copulas. The partial derivatives for $\Psi_{X|Y}^{(l)}$ are:

$$\frac{\partial\Psi_{X|Y}^{(l)}(u,v)}{\partial u} := \frac{1}{v} \frac{\partial C(u,v)}{\partial u}, \quad \text{and} \quad \frac{\partial\Psi_{X|Y}^{(l)}(u,v)}{\partial v} := \frac{1}{v} \frac{\partial C(u,v)}{\partial v} - \frac{C(u,v)}{v^2},$$

where

$$P[V \leq v | U = u] = \frac{\partial C(u,v)}{\partial u}, \quad \text{and} \quad P[U \leq u | V = v] = \frac{\partial C(u,v)}{\partial v}.$$

The functions \mathbb{M} and \mathbb{W} represent the two extreme situations of complete positive and negative dependence, where one random variable is perfectly predictable from the other. In the positive dependence situation of *co-monotonicity*, one is a monotone increasing transformation of the other, while for *counter-monotonicity* the two random variables are related by a monotone decreasing transformation. The independence case of no functional relationship is instead represented by

$$\mathbb{I}_{X|Y} := \frac{\Pi(u,v)}{v} = u, \quad \text{and} \quad \mathbb{I}_{Y|X} := \frac{\Pi(u,v)}{u} = v.$$

Indeed, given a point (u_0, v_0) in D_v , if $\Psi_{X|Y}^{(l)}(u_0, v_0) > \mathbb{I}_{X|Y}(u_0, v_0)$, then $P(X \leq x_0 | Y \leq y_0) > P(X \leq x_0)$, and if $\Psi_{X|Y}^{(l)}(u_0, v_0) < \mathbb{I}_{X|Y}(u_0, v_0)$, we have the opposite inequality $P(X \leq x_0 | Y \leq y_0) < P(X \leq x_0)$. Now, if we have instead $\Psi_{X|Y}^{(l)} = \mathbb{I}_{X|Y}$, then $\Psi_{Y|X}^{(l)} = \mathbb{I}_{Y|X}$, $P(X \leq x_0 | Y \leq y_0) = P(X \leq x_0)$, and $P(Y \leq y_0 | X \leq x_0) = P(Y \leq y_0)$.

Functions $\mathbb{I}_{X|Y}$, $\mathbb{M}_{X|Y}$, and $\mathbb{W}_{X|Y}$ are displayed in Figure 1, along with their level curves. From a geometric point of view, the function $\mathbb{I}(u, v)$ represents the cylinder with generatrix line $z = u$ and directrix the v -axis enclosed in the unit cube, which is simply a plane connecting the lower-left and the upper-right sides of the unit cube. Noting that the given plane is a *minimal surface* inside the unit cube, we can state the following theorem.

Theorem 1.2. Let $C(u, v)$ be a bivariate copula and $A(\Psi_{X|Y}^{(l)}) := \int_{\Psi_{X|Y}^{(l)}} 1 \, dS$ denote the integral of 1 over the surface $\Psi_{X|Y}^{(l)}(u, v) := C(u, v)/v$, i.e, the surface area of $\Psi_{X|Y}^{(l)}$, then we have that

$$\sqrt{2} = A(\mathbb{I}_{X|Y}) \leq A(\Psi_{X|Y}^{(l)}) \leq A(\mathbb{M}_{X|Y}) = A(\mathbb{W}_{X|Y}) = 1.708. \quad (15)$$

While it is straightforward to analytically compute the lower bound of $\sqrt{2}$, the upper bound of 1.708 was obtained numerically (although it is possible to solve one of the two integrals analytically so that the numerical integration is in just one dimension).

Theorem 1.2 suggests that the surface area of $\Psi_{X|Y}^{(l)}$ could be used as a measure of dependence. Indeed, one can define an index by normalizing the surface area $A(\Psi_{X|Y}^{(l)})$ over the interval $[0, 1]$. Of course, the same reasoning

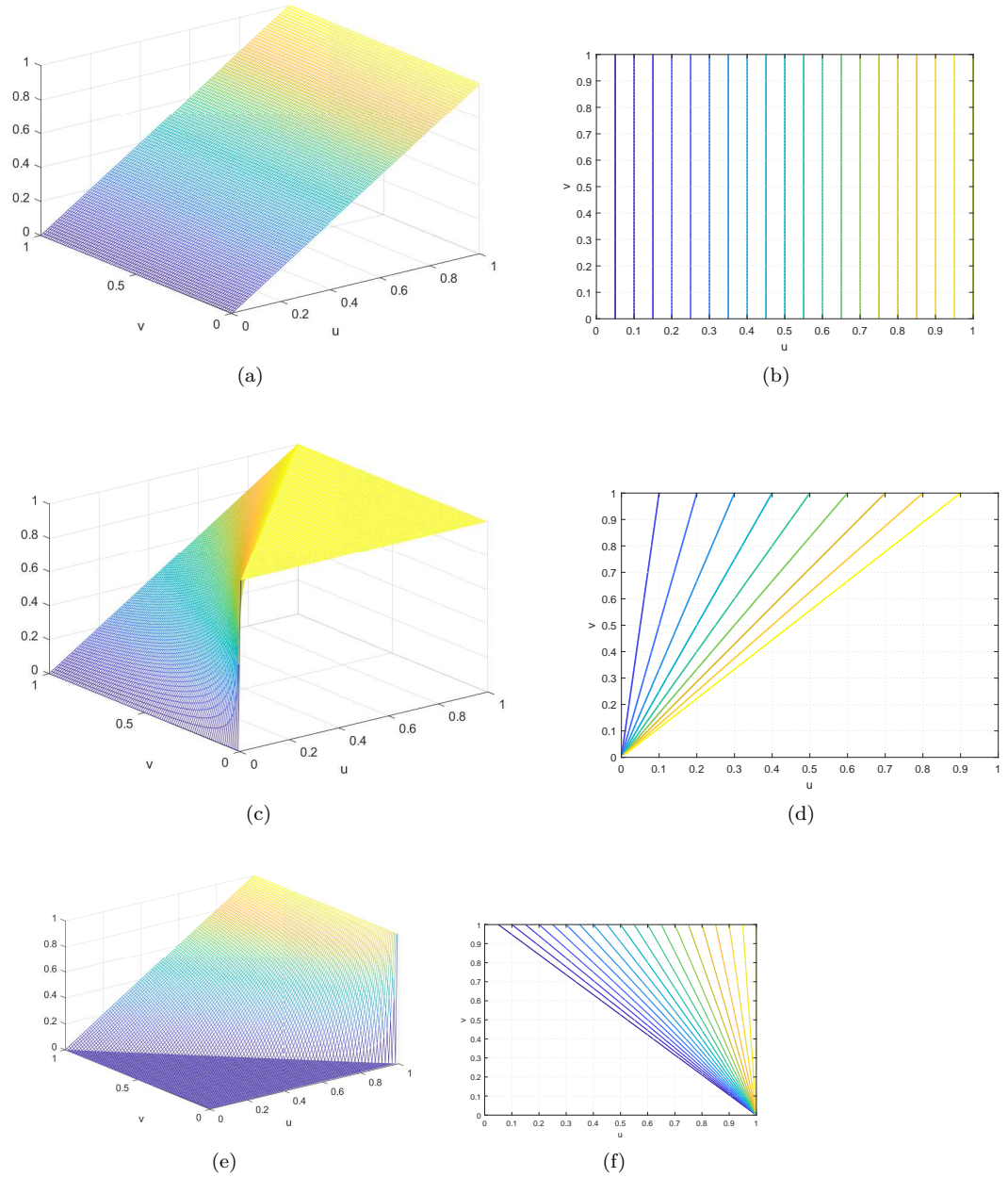


Figure 1: Lower unit square cumulative conditional probability surfaces (left panels) and their level curves (right panels) in copula space corresponding to the cases of independence ($\mathbb{I}_{X|Y}$, top panels), co-monotonicity ($\mathbb{M}_{X|Y}$, middle panels), and counter-monotonicity ($\mathbb{W}_{X|Y}$, bottom panels).

applies to $\Psi_{Y|X}^{(l)}$; furthermore, it is easy to show that $A(\mathbb{W}_{Y|X}) = A(\mathbb{W}_{X|Y})$, $A(\mathbb{M}_{Y|X}) = A(\mathbb{M}_{X|Y})$ and $A(\mathbb{I}_{Y|X}) = A(\mathbb{I}_{X|Y})$, so that we can remove subscripts. This therefore motivates the definition of $\delta_{X|Y}^{(l)}$ given below. Note that (obvious) analogous results hold for $\delta_{Y|X}^{(l)}$ defined through $\Psi_{Y|X}^{(l)}$, here and in the ensuing discussion, and we therefore omit any further allusions to it.

Definition 1.2. Let X and Y be two continuous random variables with joint distribution function H and copula C . Let $\Psi_{X|Y}^{(l)}$ and $\Psi_{Y|X}^{(l)}$ be as defined in (8). We define the lower (unit square cumulative conditional probability) measure of dependence $\delta_{X|Y}^{(l)}$ as

$$\delta_{X|Y}^{(l)} := \frac{A(\Psi_{X|Y}^{(l)}) - A(\mathbb{I})}{A(\mathbb{W}) - A(\mathbb{I})} = \frac{A(\Psi_{X|Y}^{(l)}) - A(\mathbb{I})}{A(\mathbb{M}) - A(\mathbb{I})}. \quad (16)$$

In order to more fully understand $\delta_{X|Y}^{(l)}$, consider the vector field $\nabla\Psi_{X|Y}^{(l)}$ that acts as a weight with respect to the infinitesimal area element $dudv$ in the surface integral

$$A(\Psi_{X|Y}^{(l)}) = \int_{\Psi_{X|Y}^{(l)}} \sqrt{1 + \|\nabla\Psi_{X|Y}^{(l)}(u, v)\|^2} \, dudv.$$

In the independence case we have that $\partial\Psi_{X|Y}^{(l)}(u, v)/\partial v = 0$ and $\partial\Psi_{X|Y}^{(l)}(u, v)/\partial u = 1$ for all $(x, y) \in D_v$. With respect to the upper bound of $\mathbb{M}_{X|Y}$, it is easy to see that $\partial\mathbb{M}_{X|Y}(u, v)/\partial u$ is everywhere non-negative, assuming a maximum value as $u, v \rightarrow 0$, whereas $\partial\mathbb{M}_{X|Y}(u, v)/\partial v$ is always non-positive, assuming a minimum value as $u, v \rightarrow 0$. Similarly, observe that $\partial\mathbb{W}_{X|Y}(u, v)/\partial u$ and $\partial\mathbb{W}_{X|Y}(u, v)/\partial v$ are everywhere non-negative, taking on maximum values as $u \rightarrow 1$ and $v \rightarrow 0$. These considerations imply that as the function $\Psi_{X|Y}^{(l)}$ converges toward $\mathbb{M}_{X|Y}$ or $\mathbb{W}_{X|Y}$, the value of $\|\nabla\Psi_{X|Y}^{(l)}\|$ increases, and does so at an increasingly faster rate as it approaches the point $(0, 0)$ in the case of positive dependence, and the point $(0, 1)$ in the case of negative dependence. In other words, $\delta_{X|Y}^{(l)}$ assigns increasing weight to those points (u, v) that depart from the independence case and that are either in the lower-left or lower-right portion of the domain D_v .

The next result states that $\delta_{X|Y}^{(l)}$ satisfies the properties of a *dependence measure*, as stated in Definition A.5, except for property 3 which requires symmetry with respect to conditioning; $X|Y$ giving the same measure as $Y|X$.

Theorem 1.3. The measure $\delta_{X|Y}^{(l)}$ in Definition 1.2 satisfies all the properties of a measure of dependence according to Definition A.5, except for property 3.

We argue that this is a desirable feature of the measures $\delta_{X|Y}^{(l)}$ and $\delta_{Y|X}^{(l)}$, since it more completely accounts for asymmetric dependence structures. This follows from the fact that in general $C(u, v) \neq C(v, u)$, thus implying different dependence relationships with respect to the direction of conditioning. This is clear when one realizes that *dependence* in probability theory is defined as the absence of *independence*; i.e., we have dependence every time we do not have independence. But independence, after all, is defined through conditional

probabilities, which implies that deviation from independence can arise differentially with respect to the direction of conditioning. In summary, we argue that property 3 in Definition A.5 should be excluded from the axiomatic list of dependence measures.

The fact that the normalization in Definition 1.2 is insensitive to whether co-monotonicity or counter-monotonicity is used, means that the “sign” of dependence is lost. In order to devise a measure that differentiates between positive and negative dependence structures, what is defined in the literature as a measure of *concordance*, a simple and intuitive approach is to consider the surface integral

$$S_2(\Psi_{X|Y}^{(l)}) := \int_{\Psi^{(l)}} \left[\Psi_{X|Y}^{(l)}(u, v) - \mathbb{I}_{X|Y}(u, v) \right] dS.$$

For any given point (u_0, v_0) , this integral spans the volume of the infinitesimal parallelepiped with base area $(1 + \|\nabla \Psi_{X|Y}^{(l)}\|^2)^{1/2} du_0 dv_0$ and height $|\Psi_{X|Y}^{(l)}(u, v) - \mathbb{I}_v(u, v)|$. Suitable normalization of S_2 values over the interval $[-1, 1]$, leads to the definition of the *lower* (unit square cumulative conditional probability) concordance index

$$\kappa_{X|Y}^{(l)} := \frac{2 \left[S_2(\Psi_{X|Y}^{(l)}) - S_2(\mathbb{W}) \right]}{S_2(\mathbb{M}) - S_2(\mathbb{W})} - 1, \quad (17)$$

Using similar reasoning as for Theorem 1.3, it is straightforward to show that $\kappa_{X|Y}^{(l)}$ satisfies all the properties of a measure of concordance listed in Definition A.6, except for property 3. Kendall’s tau (τ) and Spearman’s rho (ρ) are perhaps the best known measures of concordance satisfying all 7 properties.

The definition of the measures $\delta_{X|Y}^{(l)}$ and $\kappa_{X|Y}^{(l)}$ relied on the cumulative conditional probability $P(X \leq x|Y \leq y)$ in order to quantify departures from independence that occur on the *lower* triangular half of the unit square bounded by the line $u + v = 1$. Similarly, and with special relevance to the introduction of tail dependence in the next section, we can apply the ideas developed so far to devise analogous measures that focus on the *upper* triangular half, based on the conditional probability $P(X > x|Y > y)$. The development parallels the earlier, starting with the definition of corresponding subsets of the unit square

$$D_{1-v} = \{(u, v) : u \in [0, 1], v \in [0, 1]\}, \quad \text{and} \quad D_{1-u} = \{(u, v) : u \in [0, 1], v \in [0, 1]\},$$

leading to the introduction of functions $\Psi_{X|Y}^{(u)} : D_{1-v} \rightarrow [0, 1]$ and $\Psi_{Y|X}^{(u)} : D_{1-u} \rightarrow [0, 1]$,

$$\Psi_{X|Y}^{(u)}(u, v) := \frac{1 - u - v + C(u, v)}{1 - v}, \quad \Psi_{Y|X}^{(u)}(u, v) := \frac{1 - u - v + C(u, v)}{1 - u}, \quad (18)$$

which represent $P(X > x|Y > y)$ and $P(Y > y|X > x)$, respectively. It is straightforward to show that $(1 - u - v + \mathbb{W})/(1 - v)$ and $(1 - u - v + \mathbb{W})/(1 - u)$ can be obtained by respectively rotating \mathbb{W}/v and \mathbb{W}/u about the z -axis through π radians. This leads directly to the definition of the *upper* triangular half versions of (16) and (17),

$$\delta_{X|Y}^{(u)} := \frac{A(\Psi_{X|Y}^{(u)}) - A(\mathbb{I})}{A(\mathbb{W}) - A(\mathbb{I})} = \frac{A(\Psi_{X|Y}^{(u)}) - A(\mathbb{I})}{A(\mathbb{M}) - A(\mathbb{I})},$$

and

$$\kappa_{X|Y}^{(u)} = \frac{2 \left[S_2(\Psi_{X|Y}^{(u)}) - S_2(\mathbb{W}) \right]}{S_2(\mathbb{M}) - S_2(\mathbb{W})} - 1.$$

We illustrate the values of both lower and upper versions of $\kappa_{X|Y}$ along with Kendall's tau and Spearman's rho, for a select list of copulas in Tables 2 and 4. In Table 2, the copulas used are implied by the GH distributional parameters listed in Table 1, which implicitly define the copula (hence "implied"). These GH's have a relatively high number of parameters (approximately 10). Functional forms for the copulas of Table 4 can be found in Appendix C. Results are obtained with numerical integration on a structured Cartesian mesh with 10^6 points (although in some cases it may actually be possible to obtain closed formulas).

We observe that the κ measures assign more weight when the dependence, whether positive or negative, is in the extreme zones of the support. Compare for instance the value of $\kappa^{(l)}$ for the Gumbel copula with $\theta = 4$ and the Clayton copula with $\theta = 5$. These copulas have relatively close values for each of Kendall's τ and Spearman's ρ , but larger differences between their corresponding $\kappa^{(l)}$, with the value of 0.92 for the Clayton exceeding that of 0.84 for the Gumbel. The situation then reverses for $\kappa^{(u)}$, where the Clayton value of 0.73 is smaller than the 0.91 of the Gumbel. These results are consistent with the fact that the Clayton and Gumbel copulas have, respectively, Sibuya upper and lower TDCs equal to zero.

As another example, compare the Gumbel with $\theta = 4$ and the t copula with $\nu = 1$ and $\rho = 0.95$. The Gumbel has lower values of $\kappa^{(l)}$ because its Ψ function is always smaller. On the other hand, $\kappa^{(u)}$ values are very close since neither of the two $\Psi^{(u)}$ surfaces dominates the other. We can see this in Figure 2, where panel (a) displays the difference in the $\Psi_{X|Y}^{(l)}$ surfaces between Gumbel and t , whereas panel (b) shows this difference with respect to the $\Psi_{X|Y}^{(u)}$ surface. Finally, it is evident that in either the $\Psi^{(l)}$ or $\Psi^{(u)}$ case, there is generally no difference between conditioning on $X|Y$ or $Y|X$. Some Marshall copulas and asymmetric GH distributions however, provide some examples to the contrary.

An alternative definition of $\delta_{X|Y}^{(l)}$ could be achieved through the surface integral

$$S_1(\Psi_{X|Y}^{(l)}) := \int_{\Psi_{X|Y}^{(l)}} \left| \Psi_{X|Y}^{(l)}(u, v) - \mathbb{I}_{X|Y}(u, v) \right| dS,$$

whence scaling by either boundary copula would lead to the measure

$$\bar{\delta}_{X|Y}^{(l)} := \frac{S_1(\Psi_{X|Y}^{(l)})}{S_1(\mathbb{W})} = \frac{S_1(\Psi_{X|Y}^{(l)})}{S_1(\mathbb{M})}.$$

This idea paves the way for the introduction of a TDC in the next section.

2 Tail Dependence

The previous section introduced global measures that focused on summarizing the dependence structure as revealed by surface integrals of the lower and upper cumulative conditional probabilities in copula space. In this section we adapt

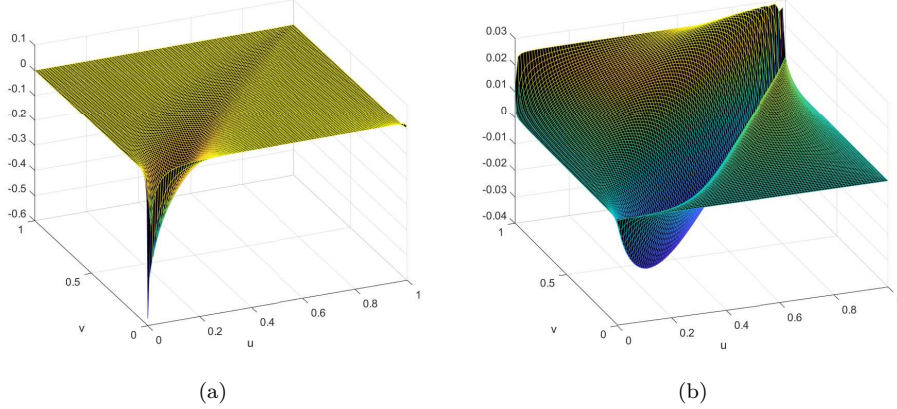


Figure 2: Panel (a): difference in the $\Psi_{X|Y}^{(l)}$ surface between the Gumbel copula with parameter $\theta = 4$ and the t copula with parameters $\nu = 1$ and $\rho = 0.95$. Panel (b): the same difference, but with respect to the surface $\Psi_{X|Y}^{(u)}$.

these measures to assess lower and upper tail dependence in extreme regions of the copula domain, leading to the definition of TDCs in similar vein to the weak (χ) and strong (λ) discussed in the Introduction.

For a function $\mathcal{Q}(u, v)$ serving as a place-holder for any of the surfaces Ψ , \mathbb{M} , \mathbb{W} , or Θ in the copula domain, define the operator $L(\cdot)$ as

$$L(\mathcal{Q}(u, v)) := -\min \left\{ \frac{\partial \mathcal{Q}(u, v)}{\partial v} \cdot \frac{\partial \mathcal{Q}(u, v)}{\partial u}, 0 \right\},$$

and the corresponding surface integral

$$\Gamma(\mathcal{Q}; p) := \int_{\mathcal{Q}} [L(\mathcal{Q}(u, v))]^p dS.$$

With this notation, observe that $L(\Psi_{X|Y}^{(l)}(u, v))$ will assume greater values as the difference $\mathbb{M}_{X|Y}(u, v) - \Psi_{X|Y}^{(l)}(u, v)$ decreases. Furthermore, as $\Psi_{X|Y}^{(l)}$ converges toward $\mathbb{M}_{X|Y}$, $L(\Psi_{X|Y}^{(l)}(u, v))$ increases faster as u and v approach zero. This ties in with the behavior of $\partial \mathbb{M}_{X|Y}(u, v)/\partial u$ as already noted in the previous section, non-negative assuming a maximum value as $u, v \rightarrow 0$, and that of $\partial \mathbb{M}_{X|Y}(u, v)/\partial v$ which is non-positive and is minimized as $u, v \rightarrow 0$. The same analysis holds for $L(\Psi_{Y|X}^{(l)})$.

We can now introduce the *lower* and *upper* TDCs defined through the normalized ratio of surface integrals,

$$\Lambda_{X|Y}^{(l)}(p) := \frac{\Gamma(\Psi_{X|Y}^{(l)}; p)}{\Gamma(\mathbb{M}_{X|Y}; p)}, \quad \text{and} \quad \Lambda_{X|Y}^{(u)}(p) = \frac{\Gamma(\Psi_{X|Y}^{(u)}; p)}{\Gamma(\mathbb{M}_{X|Y}; p)}. \quad (19)$$

Note that normalization by $\Gamma(\mathbb{W}_{X|Y}; p)$ would not result in a valid measure, as this surface integral is zero. In order to do so, one would have to modify the definition of $L(\cdot)$ by replacing $-\min$ with \max . Normalization by

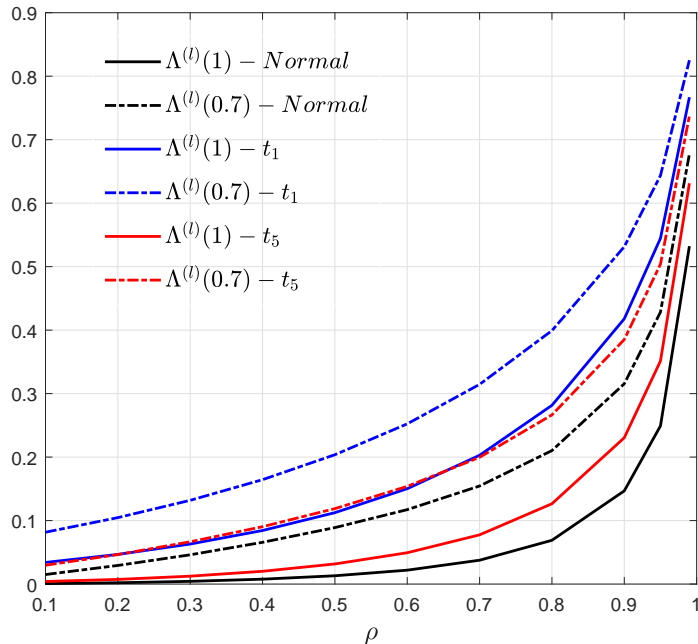


Figure 3: Lower TDC $\Lambda^{(l)}(p)$ for the Gaussian and t distributions as a function of the correlation parameter ρ .

$\Gamma(\mathbb{W}_{X|Y}; p)$ would now result in a measure of *counter-tail* (opposite) dependence, i.e., $P(X < x|Y > y)$ for small x and large y . As such, the choice of normalizing by $\Gamma(\mathbb{M}_{X|Y}; p)$ provides a measure of *co-tail* dependence (similarity), in the spirit of the weak and strong TDCs alluded to in the Introduction.

The parameter p can be used to increase, if greater than one, or to decrease, if less than one, the focus on extreme sets of the joint tail. In the case of $\Lambda^{(l)}$ this occurs when both u and v approach zero, whereas for $\Lambda^{(u)}$ it corresponds to u and v approaching one. Indeed, in the former case given that the product of $\partial\Psi_{X|Y}^{(l)}(u, v)/\partial v$ and $\partial\Psi_{X|Y}^{(l)}(u, v)/\partial u$ grows at an increasingly faster rate as $\Psi_{X|Y}^{(l)}(u, v)$ converges to $\mathbb{M}_{X|Y}(u, v)$, it will be convenient in some cases to select a value of $p < 1$ in order to re-scale $\Lambda^{(l)}$. We provide an example in Figure 3 which compares $\Lambda^{(l)}$ for the Gaussian and t distributions as a function of the correlation parameter ρ . Results for $p = 1$ ($p = 0.7$) are plotted with solid (dotted) lines. Note that for $p < 1$, the fact that $\Lambda^{(l)}(p)$ assigns less weight to the extreme regions results in a more gradual variation and smaller range in its values. Similar observations hold for $\Lambda^{(u)}$.

Table 3 displays the values of $\Lambda_{X|Y}^{(l)}(p)$, $\Lambda_{Y|X}^{(l)}(p)$, $\Lambda_{X|Y}^{(u)}(p)$, and $\Lambda_{Y|X}^{(u)}(p)$, for the GH copulas investigated in the global dependence measures (Section 1), and for the two values of $p = \{0.7, 1\}$. The last two columns in these tables correspond to the strong lower and upper TDCs, λ_l and λ_u , and provide a meaningful comparison. Results are computed via numerical integration on a uniform mesh with 10^6 points. Observe how all the chosen GH copulas have

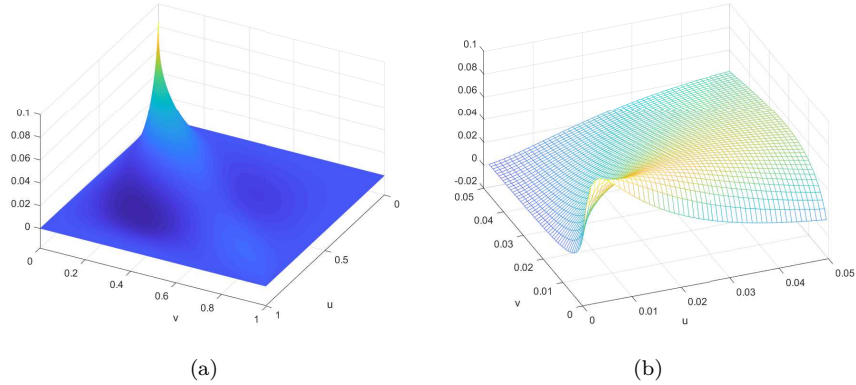


Figure 4: Difference in the $\Psi_{X|Y}^{(l)}$ surfaces for a symmetric GH distribution with parameters $\lambda = 1.5$, $\delta = 1$, $\mu = [0, 0]$, $\Delta_{12} = 0.8$, and the two different values of $\alpha = (0.5, 10)$. Panel (b) is a magnification of panel (a) in the vicinity of the origin.

positive lower and upper Λ values, but only the case of GH_2 exhibits asymptotic tail dependence ($\lambda_l = 1 = \lambda_u$).

Tables 5 and 6 display the same information, but for the non-GH copulas of Section 1. For readability Table 5 (Table 6) deals only with the case $p = 1$ ($p = 0.7$). Note how the Gumbel (Clayton) copula has a lower (upper) strong TDC of $\lambda = 0$, but the $\Lambda^{(l)}$ ($\Lambda^{(u)}$) values are increasingly different from zero as the copula parameter θ increases. The proposed Λ TDCs also correctly identify asymmetries with respect to the direction of conditioning, $X|Y$ or $Y|X$. This is the case, for example, for the Marshall copula with parameters $\{0.7, 0.9\}$, or the GH_2 and NIG_4 copulas, where the asymmetry is determined by β .

An interesting example is provided by the symmetric GH distribution with parameters $\lambda = 1.5$, $\delta = 1$, $\mu = [0, 0]$, $\Delta_{12} = 0.8$, and two different values of α . The difference between the resulting surfaces of $\Psi_{X|Y}^{(l)}$ when $\alpha = 0.5$ and $\alpha = 10$, is displayed in panel (a) of Figure 4. Panel (b) zooms in on the region close to the origin. Although the two bivariate distributions have the same lower weak TDC value of $\chi_l = 0.90$, the former has greater conditional probability in the lower-left quadrant than the latter. The values of the proposed lower TDCs on the other hand, are instead $\Lambda_{X|Y}^{(l)}(1) = 0.01$ and $\Lambda_{X|Y}^{(l)}(1) = 0.06$, respectively. (For $p = 0.7$ these values increase to 0.25 and 0.18, respectively.)

3 Simulation Study

The goal of this section is to assess the performance of maximum likelihood estimation (MLE) in parametric modeling of the proposed TDCs $\Lambda^{(l)}$ and $\Lambda^{(u)}$ defined in (19). The idea is to fit a parametric copula to the bivariate data sample, and to then compute the underlying surface integrals. In a real data scenario, this scheme would be applied to a bivariate sample of residuals obtained after appropriate modeling of the raw data. For example, in the financial

returns case study of Section 4, it is applied to the pairs of innovations resulting from (separate) ARMA-GARCH fits to each of two indices. This then justifies approximating the likelihood function in the usual way as a product of individual densities, as would be the case for an independent sample.

We simulate samples of size $n = 500$ and $n = 1000$ from a particular bivariate copula, to which a MLE algorithm is then applied to fit the parameters. This operation is replicated 1,000 times, providing an equal number of estimated values for each TDC. The following summary performance measures are then empirically computed from these 1,000 replicates: the mean, standard deviation, and mean squared error (MSE) defined as the squared bias plus variance.

Our choice of copulas encompasses three representative cases. The Gumbel copula, which has only one parameter and where the lower TDC is different from the upper; the t copula, which has two parameters, but where the lower and upper TDCs are equal; and the GH case with the parameters specified as in the second row of Table 1. The latter copula is of particular interest because it represents the asymmetric situation where the TDCs are different if computed based on $X|Y$ or $Y|X$, and also due to the fact that it has a substantially larger number of parameters to fit.

The results, presented in Table 7, confirm the good performance of MLE; a consistent and efficient estimation procedure. As expected, the GH case produces the highest MSE, bias and standard deviation, especially at the lower sample size. The stability and predictable asymptotic behavior of MLE-based estimates then furnishes the possibility of using a parametric bootstrap scheme to quantify the uncertainty in the estimates. Note that this would be the most expedient way to obtain confidence intervals for the tail dependence measures; analytical calculations involving the Hessian of the log-likelihood being infeasible due to the intractable nature of the mapping from parameter space to Λ space.

4 Case Study: Tail Dependence of Financial Indices

In this section we illustrate the computation of the proposed TDCs introduced in Section 2 on a simple financial application involving two bivariate datasets. The first consists of daily log returns of the *Dow Jones Industrial Average* (DJIA) and *Nasdaq Composite* indices, spanning the period between from 04-Jan-2004 to 25-Sep-2020. The second dataset, spanning the same period, is comprised of daily log returns of the two European indices *Ftse100* and *Dax30*, which represent, respectively, the 100 companies by capital value listed on the London Stock Exchange and the 30 companies by capital value listed on the Frankfurt Stock Exchange. The four series are plotted in Figure 5.

The goal is then to estimate $\Lambda^{(l)}$ and $\Lambda^{(u)}$ between: (i) the two American indices, and (ii) the two European indices. In order to clean rough market data from possible idiosyncratic risk due to a particular index, we use a 500-point moving window fit. That is, for each (trading) day in the time period ranging from 04-Jan-2006 to 25-Sep-2020, we fit separate univariate ARMA-GARCH models to the preceding 500 data points of each index (approximately two years). Appropriate lag orders for these conditional mean and variance

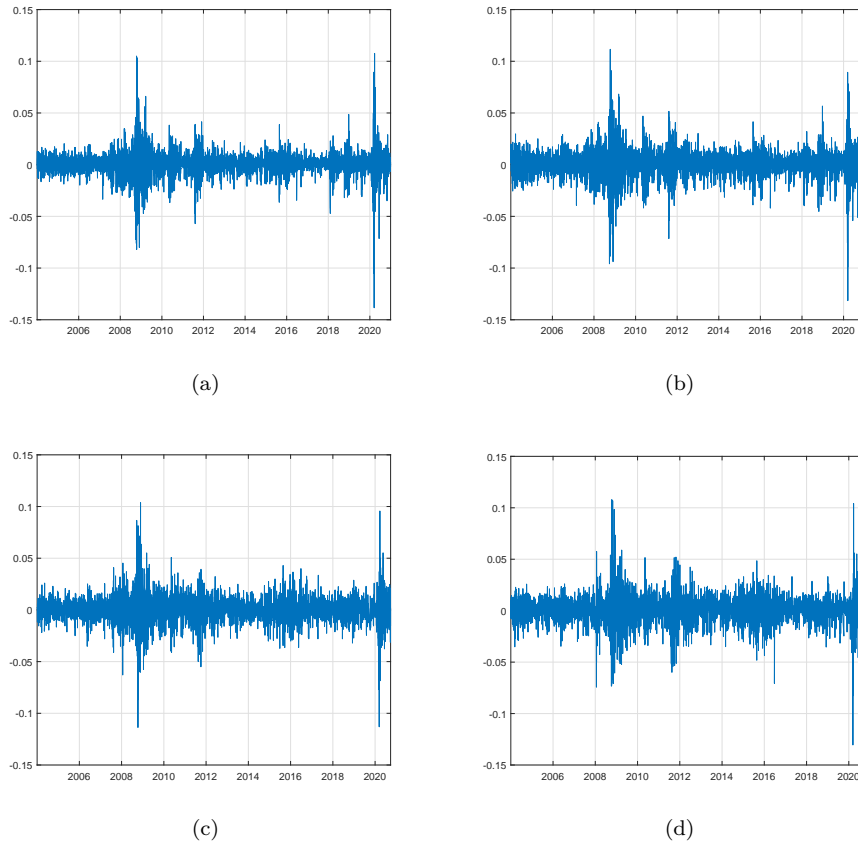


Figure 5: Daily log returns for the indices: (a) Dow Jones Industrial Average, (b) Nasdaq Composite, (c) Fitse100, and (d) Dax30.

models, were selected based on the lowest values of the information criterion BIC. All chosen models provided plausible fits, as evidenced by the lack of serial correlation in both the residuals and their squares. This then yields a bivariate vector, denoted by (X, Y) , of 500 innovations for each pair of indices at each day in the time range.

At this point we apply the MCECM algorithm [33] to fit a bivariate GH distribution to (X, Y) , from which the four TDCs $\Lambda_{X|Y}^{(l)}$, $\Lambda_{Y|X}^{(l)}$, $\Lambda_{X|Y}^{(u)}$, and $\Lambda_{Y|X}^{(u)}$ are computed (based on the implied copula) via numerical integration on a structured Cartesian mesh. To facilitate discussion, let X and Y represent respectively the DJIA and Nasdaq (American case), and Ftse100 and Dax30 (European case). The parametric bootstrap was used to construct 95% confidence bounds (using 5000 bootstrap replications).

The estimated lower TDC $\Lambda_{X|Y}^{(l)}$ for the two American indices is displayed in Figure 6, and for the two European indices in Figure 7. The other three TDCs show very similar features and are not reported, but can be obtained from the authors upon request. The estimates have a relatively narrow confidence band, as would be expected for parametric fits based on large samples, and

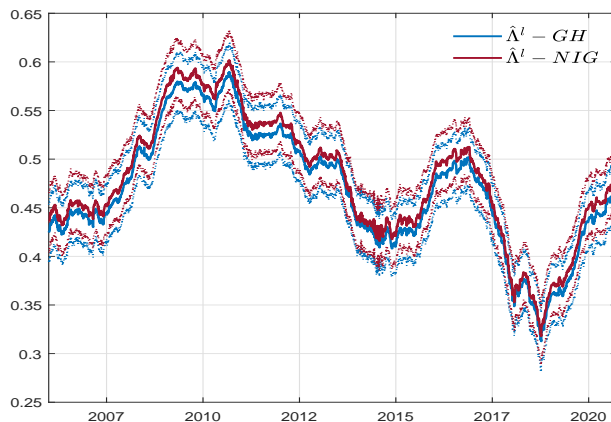


Figure 6: TDC $\hat{\Lambda}'_{X|Y}^{(l)}$ estimated from the ARMA-GARCH innovations fitted to each of the DJIA and Nasdaq returns, and based on either a GH copula (blue line) or NIG copula (red line). Corresponding 95% confidence bands are displayed as dotted lines.

exhibit trajectories that can be attributed to market conditions, with both lower and upper tail dependence increasing during periods of higher volatility. As a robustness check on the stability of our estimates against model misspecification, we replicated the procedure to estimate $\Lambda^{(l)}$ and $\Lambda^{(u)}$ for the two American indices under the hypothesis that innovations followed a NIG distribution. As shown in Figure 6, the resulting estimates (red lines) are very close to those obtained under the original GH assumption (blue lines).

Differences between the lower and upper TDCs, $\Lambda^{(l)} - \Lambda^{(u)}$, can be seen in Figure 8, for the American and European indices in panels (a) and (b), respectively. These differences range approximately from -0.02 to $+0.045$, which can be interpreted as being not significant; however, if we consider the results in Table 3, in particular the second row related to the GH_2 distribution, we can see that asymmetric structures can exist even with differences as small as 0.05 units. Our results confirm, in general, the empirical finding of [36] that lower tail dependence between stock returns tends to be stronger than the upper.

Conclusions

We have introduced alternative measures of global and tail dependence between two random variables. In the global case, the essence of the idea was to measure the surface area of the conditional cumulative probability in copula space, normalized with respect to departures from the independence copula, and scaled by the difference between the two boundary copulas of co-monotonicity (positive dependence) and counter-monotonicity (negative dependence). Two different normalization schemes lead to either a measure of *dependence* (bounded between 0 and 1) or of *concordance* (bounded between -1 and 1). The measures could be approached by cumulating probability on either the lower left or upper

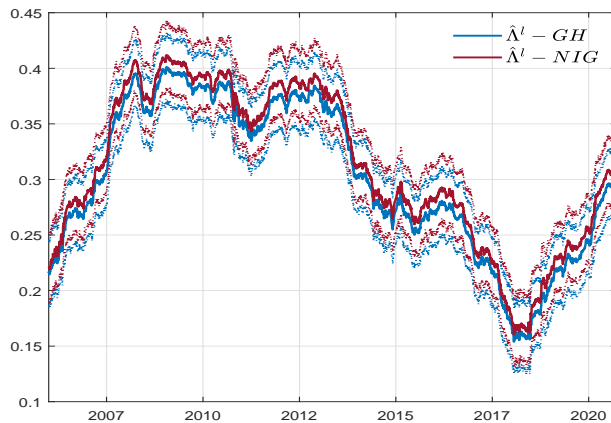


Figure 7: TDC $\Lambda_{X|Y}^{(l)}$ estimated from the ARMA-GARCH innovations fitted to each of the Ftse100 and Dax30 returns, and based on either a GH copula (blue line) or NIG copula (red line). Corresponding 95% confidence bands are displayed as dotted lines.

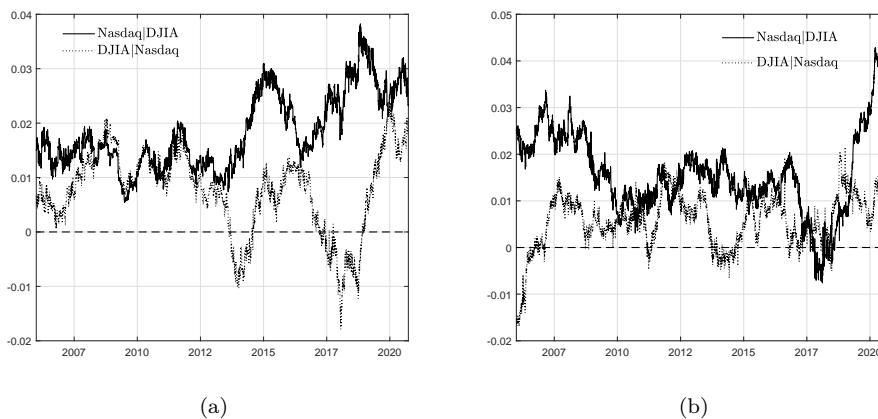


Figure 8: Panel (a): The difference $\Lambda^{(l)} - \Lambda^{(u)}$ for the cases Nasdaq|DJIA (solid) and DJIA|Nasdaq (dotted). Panel (b): The difference $\Lambda^{(l)} - \Lambda^{(u)}$ for the cases Dax30|Ftse100 (solid) and Ftse100|Dax30 (dotted).

right domain of the copula space, leading to *lower* and *upper* versions.

The TDC has been similarly derived by altering the surface integral of the global measure. In particular, we noted that the product between the two partial derivatives of the conditional cumulative probability surface is negative when the conditional probability at a given point is higher than the corresponding value in the independence case. Furthermore, the absolute value of this product increases as the copula converges toward the co-monotone case. We can then bring out the tail dependence structure by simply weighting each infinitesimal area element in the surface integral by means of a function of such a product of partial derivatives.

The measures have interesting features that make them competitive in detecting dependence in regions of the support where both random variables assume extreme values. In particular, they are able to differentiate asymmetric dependence with respect to direction of conditioning, resulting in a smoother and more refined taxonomy of global and tail dependence structures than that typically delivered by the usual measures of dependence and concordance.

More investigation on estimation procedures could of course be carried out; here we only considered the obvious parametric approach resulting from maximization of the likelihood pertaining to a choice of copula model. A fully non-parametric approach could in principle be achieved by estimating an empirical copula, such as the Beta [43] or Checkerboard [10]. Obvious computational difficulties with this route would likely arise in the calculation of the necessary surface integrals due to the necessity of performing numerical differentiation and integration.

A set of possible extensions naturally emerge from this preliminary work. Generalizations of the measures to multi-dimensional random vectors would be of particular interest. Although the theory could in principle be easily adapted in this direction by considering hyper-surface integrals, the (numerical) computational burden would increase substantially. In this regard, perhaps specialized numerical integration algorithms that take into consideration non-uniformly spaced grids could be brought to bear. It may also be fruitful to study other representations of the measures, perhaps even through characteristic functions or copula generating functions, which could in turn lead to more efficient numerical algorithms.

A Copula Theory - Basic results

In this section we summarize basic definitions and properties of copulas; references are [27] and [34]. Let S_1 and S_2 be two intervals in \mathbb{R} and let D be the planar region defined as their Cartesian product: $D = S_1 \times S_2$. Let $B = [x_1, x_2] \times [y_1, y_2]$ be a rectangular region in D and $H : \mathbb{R}^2 \supseteq D \rightarrow \mathbb{R}$ be a function of two variables. The H -volume of B is

$$V_H(B) = H(x_2, y_2) + H(x_1, y_1) - H(x_1, y_2) - H(x_2, y_1).$$

Definition A.1. The function H is called *2-increasing* if $V_H(B) \geq 0, \forall B \in D$.

Definition A.2. Suppose that $\min(S_1) = a_1$ and $\min(S_2) = a_2$. Then H is called grounded if

$$H(x, a_2) = 0 = H(a_1, y), \forall (x, y) \in D.$$

Lemma A.1. Let H be a 2-increasing function with domain D . If H is also grounded then H is also non-decreasing in each argument.

Definition A.3. Suppose that $\max(S_1) = b_1$ and $\max(S_2) = b_2$. Then H has margin functions $F : \mathbb{R} \supseteq S_1 \rightarrow \mathbb{R}$ and $G : \mathbb{R} \supseteq S_2 \rightarrow \mathbb{R}$ given by $F(x) = H(x, b_2)$ and $G(x) = H(b_1, x)$.

Definition A.4 (Bivariate Copula). Let I be the unit interval $[0, 1]$ and $I^2 = I \times I$ its Cartesian product. A bivariate copula C is a function with domain I^2 such that:

1. C is grounded and 2-increasing, and
2. $C(u, 1) = u, \forall u \in I$ and $C(1, v) = v, \forall v \in I$.

Note the basic facts that: a copula is uniformly continuous in its domain; any convex linear combination of copulas is a copula.

Theorem A.1. Let $C(u, v)$ be a copula. Then the following hold.

1. For any v in I the partial derivative $\partial C / \partial u$ exists for almost all u and $0 \leq \partial C / \partial u \leq 1$.
2. For any u in I the partial derivative $\partial C / \partial v$ exists for almost all v and $0 \leq \partial C / \partial v \leq 1$.
3. The functions $u \rightarrow \partial C / \partial v$ exist and $v \rightarrow \partial C / \partial u$ are defined and non-decreasing almost everywhere on I .

Theorem A.2 (Sklar's Theorem). Let H be a bivariate distribution function with margins F and G . Then, there exists a copula C such that for all $(x, y) \in \mathbb{R}^2$, $H(x, y) = C(F(x), G(y))$. If F and G are continuous, then C is unique. For every $(u, v) \in I^2$ we also have that $C(u, v) = H(F^{-1}(u), G^{-1}(v))$.

Theorem A.3. Let X and Y be two continuous random variables with distribution functions F and G , respectively, and joint distribution function H . Let C be the copula obtained as $C(u, v) = H(F^{-1}(u), G^{-1}(v))$. Then X and Y are independent if and only if $C(u, v) = uv$.

Theorem A.4 (Fréchet-Hoeffding Bounds). Define the functions $W : I^2 \rightarrow I$ and $M : I^2 \rightarrow I$ as, $W(u, v) := \max(u + v - 1, 0)$, and $M(u, v) := \min(u, v)$. Then, for every copula C we have that

$$W(u, v) \leq C(u, v) \leq M(u, v), \quad \text{for all } (u, v) \in I^2.$$

Theorem A.5. Let X and Y be continuous random variables with copula $C_{X,Y}$. If α and β are strictly increasing functions on the supports of X and Y , respectively, then $C_{\alpha(X), \beta(Y)} = C_{X,Y}$. Thus $C_{X,Y}$ is invariant under strictly increasing transformations of X and Y .

Definition A.5 (Measure of Dependence). A numeric measure δ of association between two continuous random variables X and Y whose copula is C , is a measure of *dependence* if it satisfies the following properties (we write $\delta_{X,Y}$ or δ_C when needed):

1. δ is defined for every pair X, Y of continuous random variables;
2. $0 \leq \delta_{X,Y} \leq 1$;
3. $\delta_{X,Y} = \delta_{Y,X}$
4. $\delta_{X,Y} = 0$ if and only if X and Y are independent;
5. $\delta_{X,Y} = 1$ if and only if each of X and Y is almost surely a strictly monotone function of the other;
6. if α and β are almost surely strictly monotone functions on the supports of X and Y , respectively, then $\delta_{\alpha(X),\beta(Y)} = \delta_{X,Y}$
7. if $\{(X_n, Y_n)\}$ is a bivariate sequence of continuous random variables with copulas C_n , and if $\{C_n\}$ converges pointwise to C , then $\lim_{n \rightarrow \infty} \delta_{C_n} = \delta_C$.

An example of a dependence measure is given by the Schweizer and Wolff's σ :

$$\sigma = 12 \int_{I^2} |C(u, v) - uv| dudv. \quad (20)$$

Definition A.6 (Measure of Concordance). A numeric measure κ of association between two continuous random variables X and Y whose copula is C , is a measure of *concordance* if it satisfies the following properties (we write $\kappa_{X,Y}$ or κ_C when needed):

1. κ is defined for every pair (X, Y) of continuous random variables;
2. $-1 \leq \kappa_{X,Y} \leq 1$; $\kappa_{X,X} = 1$ and $\kappa_{X,-X} = -1$
3. $\kappa_{X,Y} = \kappa_{Y,X}$
4. if X and Y are independent, then $\kappa_{X,Y} = \kappa_{\Pi} = 0$;
5. $\kappa_{-X,Y} = \kappa_{X,-Y} = -\kappa_{X,Y}$
6. if C_1 and C_2 are copulas such that $C_1 \prec C_2$, then $\kappa_{C_1} \leq \kappa_{C_2}$
7. if $\{(X_n, Y_n)\}$ is a bivariate sequence of continuous random variables with copulas C_n , and if $\{C_n\}$ converges pointwise to C , then $\lim_{n \rightarrow \infty} \kappa_{C_n} = \kappa_C$.

Popular measures of concordance are Kendall's tau

$$\tau_C = 4 \int_{I^2} C(u, v) dC(u, v) - 1 = 1 - 4 \int_{I^2} \frac{\partial}{\partial u} C(u, v) \frac{\partial}{\partial v} C(u, v) dudv,$$

and Spearman's rho

$$\rho_C = 12 \int_{I^2} uv dC(u, v) - 3 = 12 \int_{I^2} C(u, v) dudv - 3 = 12 \int_{I^2} [C(u, v) - uv] dudv.$$

Thus ρ_C is a measure of "average distance" between the distributions of X and Y (as represented by C) and independence (as represented by the copula Π).

B Proofs

Theorem 1.2

The last equality in (15) is trivial:

$$\int_{\mathbb{I}_{X|Y}} 1 \, dS = \int_0^1 \int_0^1 \sqrt{2} \, dudv = \sqrt{2}$$

. It is also easy to prove that $\int_{\mathbb{W}} 1 \, dS = \int_{\mathbb{M}} 1 \, dS$. Now, for the terms in the first integral

$$\mathbb{W}_{X|Y} = \frac{1}{2v} (|u + v - 1| + u + v - 1), \quad (21)$$

$$\frac{\partial \mathbb{W}_{X|Y}}{\partial u} = \frac{1}{2v} \cdot [\text{sign}(u + v - 1) + 1], \quad (22)$$

$$\frac{\partial \mathbb{W}_{X|Y}}{\partial v} = \frac{1}{2v} \cdot \left[\text{sign}(u + v - 1) + 1 - \frac{|u + v - 1| + u + v - 1}{v} \right]. \quad (23)$$

When $u + v + 1 < 0$ then $\partial \mathbb{W}_v / \partial u = \partial \mathbb{W}_v / \partial v = 0$, so we can write

$$\int_{\mathbb{W}_{X|Y}} 1 \, dS = \int_0^1 \int_0^{1-u} 1 \, dvdu + \int_0^1 \int_{1-u}^1 \sqrt{\frac{v^4 + v^2 + (1-u)^2}{v^4}} \, dvdu. \quad (24)$$

Consider now the second integral terms

$$\mathbb{M}_{X|Y} = \frac{1}{2v} (u + v - |u - v|), \quad (25)$$

$$\frac{\partial \mathbb{M}_{X|Y}}{\partial u} = \frac{1}{2v} [-\text{sign}(u - v) + 1], \quad (26)$$

$$\frac{\partial \mathbb{M}_{X|Y}}{\partial v} = -\frac{1}{2v^2} [u + v - |u - v|] + \frac{1}{2v} [1 + \text{sign}(u - v)]. \quad (27)$$

When $v < u$ then $\partial \mathbb{M}_{X|Y} / \partial u = \partial \mathbb{M}_{X|Y} / \partial v = 0$, so we can write

$$\int_{\mathbb{M}_{X|Y}} 1 \, dS = \int_0^1 \int_0^u 1 \, dvdu + \int_0^1 \int_u^1 \sqrt{\frac{v^4 + v^2 + u^2}{v^4}} \, dvdu. \quad (28)$$

We just need to define the simple transformation $w = 1 - u$ in order to rewrite the surface integral for $\mathbb{W}_{X|Y}$ as

$$\int_0^1 \int_0^{1-w} 1 \, dvdw + \int_0^1 \int_w^1 \sqrt{\frac{v^4 + v^2 + w^2}{v^4}} \, dvdw,$$

which coincides with the integral for $\mathbb{M}_{X|Y}$. In order to prove that $\int_{\mathbb{M}_{X|Y}} dS \geq \int_{\Psi_{X|Y}^{(l)}} dS$, we observe that for each (u_0, v_0) , the distance $|\Psi_{Y|X}^{(l)}(u_0, v_0) - \mathbb{I}_{X|Y}(u_0, v_0)|$ is maximized with $\Psi_{Y|X}^{(l)} = \mathbb{W}_{X|Y}$ or $\Psi_{Y|X}^{(l)} = \mathbb{M}_{X|Y}$. Given that the boundary $\partial\Omega_1$ is common to all the surfaces $\Psi_{Y|X}^{(l)}$, the inequality must hold.

Theorem 1.3

1. If X and Y are continuous they admit a unique continuous copula C . The surface area of a continuous function $f : \mathbb{R} \rightarrow \mathbb{R}$ is well-defined.
2. Relationships $0 \leq \delta_{X|Y}^{(l)} \leq 1$ follow directly from inequalities in Theorem 1.1.
3. Property 3 is satisfied, in general, if C is a symmetric copula.
4. $\delta_{X|Y}^{(l)} = 0$ if and only if $A(\Psi_{X|Y}^{(l)}) = A(\mathbb{I})$, but since $\Phi_{X|Y}$ is a minimal surface area, in order to have $A(\Psi_{X|Y}^{(l)}) = A(\mathbb{I})$ we must have $\Psi_{X|Y} = \mathbb{I}$.
5. $\delta_{X|Y}^{(l)} = 1$ only if $A(\Psi_{X|Y}^{(l)}) = A(\mathbb{W})$ or $A(\Psi_{X|Y}^{(l)}) = A(\mathbb{M})$. We know that when X and Y are continuous "Y is almost surely an increasing function of X" if and only if the copula of X and Y is \mathbb{M} , and "Y is almost surely a decreasing function of X" if and only if the copula of X and Y is \mathbb{W} . Thus, $\delta_{X|Y}^{(l)} = 1$ if and only if each X and Y is almost surely a strictly monotone function of the other.
6. Follows directly from theorem A.5.
7. This is equivalent to proving that

$$\lim_{n \rightarrow \infty} \int_0^1 \int_0^1 \sqrt{1 + \|\nabla \Psi_{n,v}^{(l)}\|^2} dvdu = \int_0^1 \int_0^1 \sqrt{1 + \|\nabla \Psi_v^{(l)}\|^2} dvdu,$$

where $\Psi_{X|Y,n}^{(l)} := C_n/v$, which follows from the fact that a continuous copula is uniformly continuous.

C Generalized Hyperbolic Distribution and Other Copulas

The bivariate Generalized Hyperbolic (GH) distribution, due to [2], is defined as follows. Let Δ be a real-valued, positive semidefinite (2×2) matrix and let $\lambda \in \mathbb{R}$, $\alpha, \delta \in \mathbb{R}_+$, and $\beta, \mu \in \mathbb{R}^2$ be a set of parameters satisfying the following alternative constraints:

$$\begin{aligned} \delta \geq 0, 0 \leq \sqrt{\beta' \Delta \beta} < \alpha, & \quad \text{if } \lambda > 0, \\ \delta > 0, 0 \leq \sqrt{\beta' \Delta \beta} < \alpha, & \quad \text{if } \lambda = 0, \\ \delta > 0, 0 \leq \sqrt{\beta' \Delta \beta} \leq \alpha, & \quad \text{if } \lambda < 0. \end{aligned}$$

The GH density of the bivariate continuous random vector $Z = [X, Y]$ is then defined as:

$$\begin{aligned} h(z; \lambda, \alpha, \beta, \delta, \mu, \Delta) &= \frac{(\alpha^2 - \beta' \Delta \beta)^{\frac{\lambda}{2}}}{(2\pi)^{\frac{2}{2}} \sqrt{|\Delta|} \alpha^{\lambda - \frac{2}{2}} \delta^\lambda K_\lambda \left(\delta \sqrt{\alpha^2 - \beta' \Delta \beta} \right)} \\ &\times \left((z - \mu)' \Delta^{-1} (z - \mu) + \delta^2 \right)^{\frac{(\lambda - \frac{2}{2})}{2}} \\ &\times K_{\lambda-1} \left(\alpha \sqrt{(z - \mu)' \Delta^{-1} (z - \mu) + \delta^2} \right) e^{\beta'(z - \mu)}, \quad (29) \end{aligned}$$

where $|\Delta|$ is the determinant of Δ , and K_ν is the modified Bessel function of the third kind with index ν . The GH class contains important distribution families: the *multivariate Normal Inverse Gaussian* (NIG) for $\lambda = -1/2$, the *multivariate Variance-Gamma* (VG) if $\lambda > 0$ and $\delta \rightarrow \infty$; in the case in which $\beta = [0, 0]$, the random vector Z is elliptically contoured and its distribution is called multivariate symmetric GH. The *multivariate scaled and shifted t-distribution* with -2λ degrees of freedom is part of the symmetric sub-class, and is attained for $\lambda < 0$ and $\alpha \rightarrow 0$. The *Multivariate Normal* distribution is the limiting case of $\alpha \rightarrow \infty$, $\delta \rightarrow \infty$, and $\delta/\alpha \rightarrow \sigma^2 < \infty$. A particular GH distribution will induce a specific (implied) copula, which in general can only be numerically computed.

Functional forms for other copula used in this paper are as follows.

- Fréchet Copula, [15]

$$C(u, v; \alpha, \beta) = \alpha M(u, v) + (1 - \alpha - \beta)\Pi(u, v) + \beta W(u, v) \quad (30)$$

for $\alpha, \beta \in [0, 1]$ and $\alpha + \beta \leq 1$

- Mardia Copula, [30]

$$C(u, v; \theta) = \frac{\theta^2(1+\theta)}{2}M(u, v) + (1-\theta^2)\Pi(u, v) + \frac{\theta^2(1-\theta)}{2}W(u, v) \quad (31)$$

for $\theta \in [-1, 1]$

- Cuadras-Augé Copula, [8]

$$C(u, v; \theta) = [\min(u, v)^\theta]^\theta [uv]^{1-\theta} \quad (32)$$

for $\theta \in [0, 1]$

- Gumbel-Hougaard Copula, [18] [24]

$$C(u, v; \theta) = \exp \left[- \left[(-\ln u)^\theta + (-\ln v)^\theta \right]^{\frac{1}{\theta}} \right] \quad (33)$$

for $\theta \in [-1, 1]$

- Ali-Mikhail - Haq Copula, [26]

$$C(u, v; \theta) = \frac{uv}{1 - \theta(1-u)(1-v)} \quad (34)$$

for $\theta \in [-1, 1]$

- Clayton Copula, [7]

$$C(u, v; \theta) = \max(u^{-\theta} + v^{-\theta} - 1, 0)^{-\frac{1}{\theta}} \quad (35)$$

for $\theta \in [-1, 0) \cup (0, \infty)$

- Frank Copula, [14]

$$C(u, v; \theta) = -\frac{1}{\theta} \ln \left[1 + \frac{(e^{-\theta u} - 1)(e^{-\theta v} - 1)}{e^{-\theta} - 1} \right] \quad (36)$$

for $\theta \in \mathbb{R}$

- Marshall and Olkin Copula, [31] and [32]

$$C(u, v; \theta) = \min(u^{1-\alpha}v, uv^{1-\beta}) \quad (37)$$

for $\alpha > 0$ and $\beta < 1$

Tables

Copula	λ	α	β_1	β_2	δ	μ_1	μ_2	$\Delta_{1,1}$	$\Delta_{1,2}$	$\Delta_{2,2}$
GH ₁	1.50	1.10	0.00	0.00	1	0	0	2.29	2.06	2.29
GH ₂	1.50	0.80	-0.40	0.30	1	0	0	2.29	2.06	2.29
GH ₃	1.00	1.30	0.00	0.00	1	0	0	1.77	1.57	1.96
GH ₄	1.00	1.30	-0.40	-0.30	1	0	0	3.43	0.69	0.43
NIG ₁	-0.50	1.20	0.00	0.00	1	0	0	1.77	1.57	1.96
NIG ₂	-0.50	1.20	-0.40	-0.30	1	0	0	1.77	1.57	1.96
NIG ₃	-0.50	1.20	-0.40	-0.30	1	0	0	3.43	0.69	0.43
NIG ₄	-0.50	1.20	-0.40	0.30	1	0	0	3.43	0.69	0.43
VG ₁	0.80	1.30	0.00	0.00	0	0	0	1.77	1.57	1.96
VG ₂	0.80	1.30	-0.40	-0.30	0	0	0	1.77	1.57	1.96
VG ₃	0.50	1.10	-0.40	-0.30	0	0	0	1.77	1.57	1.96
VG ₄	0.50	1.10	-0.40	-0.30	0	0	0	3.43	0.69	0.43

Table 1: Selected bivariate GH distributions.

Copula	$\kappa_{X Y}^{(l)}$	$\kappa_{Y X}^{(l)}$	$\kappa_{X Y}^{(u)}$	$\kappa_{Y X}^{(u)}$	τ	ρ
GH ₁	0.85	0.85	0.85	0.85	0.71	0.87
GH ₂	0.85	0.86	0.83	0.82	0.70	0.86
GH ₃	0.78	0.78	0.78	0.78	0.64	0.81
GH ₄	0.71	0.71	0.59	0.58	0.53	0.70
NIG ₁	0.78	0.78	0.78	0.78	0.64	0.81
NIG ₂	0.89	0.89	0.80	0.80	0.71	0.87
NIG ₃	0.67	0.67	0.53	0.52	0.47	0.63
NIG ₄	0.55	0.54	0.45	0.47	0.39	0.53
VG ₁	0.78	0.78	0.78	0.78	0.64	0.80
VG ₂	0.91	0.91	0.82	0.82	0.76	0.90
VG ₃	0.94	0.94	0.84	0.84	0.80	0.92
VG ₄	0.77	0.79	0.59	0.55	0.58	0.74

Table 2: Values of upper and lower concordance measure κ , Kendall's τ , and Spearman's ρ , computed for the implied GH copulas of Table 1.

Copula	$\Lambda_{X Y}^{(l)}$		$\Lambda_{Y X}^{(l)}$		$\Lambda_{X Y}^{(u)}$		$\Lambda_{Y X}^{(u)}$		λ_l	λ_u
	1	0.7	1	0.7	1	0.7	1	0.7		
p	1	0.7	1	0.7	1	0.7	1	0.7	0	0
GH ₁	0.19	0.36	0.19	0.36	0.19	0.36	0.19	0.36	0	0
GH ₂	0.23	0.40	0.19	0.35	0.13	0.29	0.19	0.35	1	1
GH ₃	0.13	0.28	0.13	0.28	0.13	0.28	0.13	0.28	0	0
GH ₄	0.12	0.27	0.10	0.25	0.01	0.06	0.02	0.10	0	0
NIG ₁	0.14	0.30	0.14	0.30	0.14	0.30	0.14	0.30	0	0
NIG ₂	0.37	0.52	0.36	0.51	0.09	0.23	0.09	0.24	0	0
NIG ₃	0.16	0.30	0.13	0.27	0.01	0.06	0.02	0.10	0	0
NIG ₄	0.09	0.23	0.05	0.15	0.01	0.05	0.03	0.13	0	0
VG ₁	0.14	0.30	0.14	0.30	0.14	0.30	0.18	0.32	0	0
VG ₂	0.33	0.50	0.33	0.50	0.09	0.24	0.09	0.25	0	0
VG ₃	0.42	0.58	0.38	0.56	0.09	0.24	0.11	0.26	0	0
VG ₄	0.11	0.28	0.15	0.32	0.01	0.06	0.01	0.09	0	0

Table 3: Values of upper and lower tail dependence measure Λ computed for the implied GH copulas of Table 1, and for two choices of the focus parameter p . The last two columns list also the upper and lower strong TDC λ . Results are obtained with numerical integration on a uniform mesh with 10^6 points.

Copula	Param	$\kappa_{X Y}^{(l)}$	$\kappa_{Y X}^{(l)}$	$\kappa_{X Y}^{(u)}$	$\kappa_{Y X}^{(u)}$	τ	ρ
Frechet	0.3, 0.7	-0.40	-0.40	-0.40	-0.40	-0.39	-0.41
Frechet	0.5, 0.5	0.00	0.00	0.00	0.00	0.00	0.01
Frechet	0.7, 0.3	0.40	0.40	0.40	0.40	0.40	0.39
Gumbel	4	0.84	0.84	0.91	0.91	0.75	0.90
Gumbel	6	0.91	0.91	0.96	0.96	0.83	0.95
Gumbel	10	0.96	0.96	0.99	0.99	0.90	0.97
Clayton	1	0.55	0.55	0.36	0.36	0.34	0.47
Clayton	2	0.75	0.75	0.53	0.53	0.50	0.67
Clayton	5	0.92	0.92	0.73	0.73	0.72	0.87
Clayton	10	0.97	0.97	0.84	0.84	0.83	0.95
Clayton	30	1.00	1.00	0.94	0.94	0.94	0.98
Frank	1.5	0.20	0.20	0.20	0.20	0.17	0.23
Frank	5	0.55	0.55	0.55	0.55	0.46	0.63
Frank	15	0.84	0.84	0.84	0.84	0.76	0.92
Ali	0.5	0.17	0.17	0.15	0.15	0.13	0.18
Ali	1	0.55	0.55	0.36	0.36	0.34	0.47
Mardia	-0.9	-0.71	-0.71	-0.71	-0.71	-0.68	-0.74
Mardia	0.9	0.71	0.71	0.71	0.71	0.68	0.72
Cuadras	0.5	0.35	0.35	0.41	0.41	0.34	0.42
Cuadras	0.8	0.67	0.67	0.74	0.74	0.67	0.74
Gaussian	0.5	0.44	0.44	0.44	0.44	0.33	0.47
Gaussian	0.7	0.62	0.62	0.62	0.62	0.49	0.67
Gaussian	0.9	0.85	0.85	0.85	0.85	0.71	0.88
Gaussian	0.95	0.92	0.92	0.92	0.92	0.80	0.93
Marshall	0.5, 0.5	0.35	0.35	0.41	0.41	0.34	0.42
Marshall	0.6, 0.1	0.13	0.09	0.12	0.15	0.10	0.12
Marshall	0.7, 0.9	0.68	0.62	0.71	0.76	0.65	0.72
t	0.50, 4	0.42	0.42	0.42	0.42	0.33	0.46
t	0.90, 4	0.85	0.85	0.85	0.85	0.71	0.87
t	0.95, 4	0.92	0.92	0.92	0.92	0.80	0.93
t	0.50, 2	0.42	0.42	0.42	0.42	0.33	0.44
t	0.90, 2	0.85	0.85	0.85	0.85	0.71	0.86
t	0.95, 2	0.92	0.92	0.92	0.92	0.80	0.92
t	0.50, 1	0.41	0.41	0.41	0.41	0.34	0.42
t	0.90, 1	0.83	0.83	0.83	0.83	0.71	0.83
t	0.95, 1	0.90	0.90	0.90	0.90	0.80	0.90

Table 4: Values of upper and lower concordance measure κ , Kendall's τ , and Spearman's ρ , computed for the selection of non-GH copulas discussed in Appendix C. Results are obtained with numerical integration on a structured Cartesian mesh with 10^6 points.

Copula	Param	$\Lambda_{X Y}^{(l)}(1.0)$	$\Lambda_{Y X}^{(l)}(1.0)$	$\Lambda_{X Y}^{(u)}(1.0)$	$\Lambda_{Y X}^{(u)}(1.0)$	λ_l	λ_u
Frechet	0.3, 0.7	0.03	0.03	0.03	0.03	0.3	0.3
Frechet	0.5, 0.5	0.13	0.13	0.13	0.13	0.5	0.5
Frechet	0.7, 0.3	0.34	0.34	0.34	0.34	0.7	0.7
Gumbel	1	0.00	0	0.09	0.09	0	0.41
Gumbel	4	0.07	0.07	0.48	0.48	0	0.81
Gumbel	6	0.15	0.15	0.62	0.62	0	0.88
Gumbel	10	0.29	0.29	0.77	0.77	0	0.93
Clayton	1	0.14	0.14	0	0	0.50	0
Clayton	2	0.32	0.32	0	0	0.71	0
Clayton	5	0.61	0.61	0	0	0.87	0
Clayton	10	0.78	0.78	0.01	0.01	0.93	0
Clayton	30	0.92	0.92	0.02	0.02	0.98	0
Frank	5	0	0	0	0	0	0
Frank	15	0.01	0.01	0.01	0.01	0	0
Cuadras	0.2	0	0	0.01	0.01	0	0.20
Cuadras	0.5	0	0	0.13	0.13	0	0.50
Cuadras	0.8	0.04	0.04	0.51	0.51	0	0.80
Marshall	0.1, 0.6	0.00	0.00	0.17	0.00	0	0.10
Marshall	0.5, 0.5	0.00	0.00	0.13	0.13	0	0.50
Marshall	0.6, 0.1	0.00	0.00	0.00	0.17	0	0.10
Marshall	0.7, 0.9	0.01	0.15	0.65	0.30	0	0.70
Gaussian	0.700	0.04	0.04	0.04	0.04	0.00	0.00
Gaussian	0.900	0.15	0.15	0.15	0.15	0.00	0.00
Gaussian	0.950	0.25	0.25	0.25	0.25	0.00	0.00
Gaussian	0.990	0.53	0.53	0.53	0.53	0.00	0.00
t	0.500, 2	0.07	0.07	0.07	0.07	0.42	0.42
t	0.900, 2	0.33	0.33	0.33	0.33	0.73	0.73
t	0.950, 2	0.46	0.46	0.46	0.46	0.81	0.81
t	0.500, 1	0.11	0.11	0.11	0.11	0.56	0.56
t	0.900, 1	0.42	0.42	0.42	0.42	0.80	0.80
t	0.950, 1	0.54	0.54	0.54	0.54	0.86	0.86

Table 5: Values of upper and lower tail dependence measure Λ computed for the non-GH copulas discussed in Appendix C. The value of the focus parameter is set at $p = 1$. The last two columns list also the upper and lower strong TDC λ . Results are obtained with numerical integration on a uniform mesh with 10^6 points.

Copula	Param	$\Lambda_{X Y}^{(l)}(0.7)$	$\Lambda_{Y X}^{(l)}(0.7)$	$\Lambda_{X Y}^{(u)}(0.7)$	$\Lambda_{Y X}^{(u)}(0.7)$	λ_l	λ_u
Frechet	0.3, 0.7	0.06	0.06	0.06	0.06	0.30	0.3
Frechet	0.5, 0.5	0.19	0.19	0.19	0.19	0.50	0.5
Frechet	0.7, 0.3	0.43	0.43	0.43	0.43	0.70	0.7
Gumbel	1.5	0.05	0.05	0.21	0.21	0.00	0.41
Gumbel	4	0.22	0.22	0.60	0.60	0.00	0.81
Gumbel	6	0.33	0.33	0.72	0.72	0.00	0.88
Gumbel	10	0.48	0.48	0.83	0.83	0.00	0.93
Clayton	1	0.27	0.27	0.02	0.02	0.50	0.0
Clayton	2	0.44	0.44	0.04	0.04	0.71	0.0
Clayton	5	0.69	0.69	0.06	0.06	0.87	0.0
Clayton	10	0.83	0.83	0.09	0.09	0.93	0.0
Clayton	30	0.94	0.94	0.17	0.17	0.98	0.0
Frank	5	0.05	0.05	0.05	0.05	0.00	0.0
Frank	15	0.10	0.10	0.10	0.10	0.00	0.0
Cuadras	0.2	0.01	0.01	0.04	0.04	0.00	0.2
Cuadras	0.5	0.03	0.03	0.21	0.21	0.00	0.5
Cuadras	0.8	0.16	0.16	0.59	0.59	0.00	0.8
Marshall	0.1, 0.6	0.00	0.04	0.29	0.01	0.00	0.1
Marshall	0.5, 0.5	0.03	0.03	0.21	0.21	0.00	0.5
Marshall	0.6, 0.1	0.04	0.00	0.01	0.29	0.00	0.1
Marshall	0.7, 0.9	0.08	0.31	0.73	0.43	0.00	0.7
Gaussian	0.700	0.15	0.15	0.15	0.15	0.00	0.00
Gaussian	0.900	0.32	0.32	0.32	0.32	0.00	0.00
Gaussian	0.950	0.43	0.43	0.43	0.43	0.00	0.00
Gaussian	0.990	0.68	0.68	0.68	0.68	0.00	0.00
t	0.500, 2	0.16	0.16	0.16	0.16	0.42	0.42
t	0.900, 2	0.46	0.46	0.46	0.46	0.73	0.73
t	0.950, 2	0.58	0.58	0.58	0.58	0.81	0.81
t	0.500, 1	0.20	0.20	0.20	0.20	0.56	0.56
t	0.900, 1	0.53	0.53	0.53	0.53	0.80	0.80
t	0.950, 1	0.64	0.64	0.64	0.64	0.86	0.86

Table 6: Values of upper and lower tail dependence measure Λ computed for the non-GH copulas discussed in Appendix C. The value of the focus parameter is set at $p = 0.7$. The last two columns list also the upper and lower strong TDC λ . Results are obtained with numerical integration on a uniform mesh with 10^6 points.

Distribution	Measure	Value	$n = 500$			$n = 1000$		
			mean	std. dev.	MSE	mean	std. dev.	MSE
Gumbel	$\Lambda_{Y X}^{(l)}$	0.48	0.484	0.011	$1.241 \cdot 10^{-4}$	0.483	0.008	$6.443 \cdot 10^{-5}$
	$\Lambda_{X Y}^{(l)}$	0.48	0.484	0.011	$1.241 \cdot 10^{-4}$	0.483	0.008	$6.443 \cdot 10^{-5}$
	$\Lambda_{Y X}^{(u)}$	0.83	0.828	0.0064	$4.157 \cdot 10^{-4}$	0.827	0.0046	$2.125 \cdot 10^{-5}$
	$\Lambda_{X Y}^{(u)}$	0.83	0.828	0.0064	$4.157 \cdot 10^{-4}$	0.827	0.0046	$2.125 \cdot 10^{-5}$
GH_2	$\Lambda_{Y X}^{(l)}$	0.40	0.372	0.018	$3.465 \cdot 10^{-4}$	0.392	0.012	$1.659 \cdot 10^{-4}$
	$\Lambda_{X Y}^{(l)}$	0.35	0.346	0.017	$1.101 \cdot 10^{-3}$	0.351	0.011	$2.500 \cdot 10^{-4}$
	$\Lambda_{Y X}^{(u)}$	0.29	0.313	0.019	$2.803 \cdot 10^{-4}$	0.301	0.011	$1.433 \cdot 10^{-4}$
	$\Lambda_{X Y}^{(u)}$	0.35	0.3451	0.016	$2.206 \cdot 10^{-3}$	0.348	0.013	$3.231 \cdot 10^{-4}$
t	$\Lambda_{Y X}^{(l)}$	0.30	0.2994	0.0158	$2.501 \cdot 10^{-4}$	0.3002	0.0119	$1.413 \cdot 10^{-4}$
	$\Lambda_{X Y}^{(l)}$	0.30	0.2994	0.0158	$2.501 \cdot 10^{-4}$	0.3002	0.0119	$1.413 \cdot 10^{-4}$
	$\Lambda_{Y X}^{(u)}$	0.30	0.2994	0.0157	$2.495 \cdot 10^{-4}$	0.3004	0.0119	$1.433 \cdot 10^{-4}$
	$\Lambda_{X Y}^{(u)}$	0.30	0.2994	0.0157	$2.495 \cdot 10^{-4}$	0.3004	0.0119	$1.433 \cdot 10^{-4}$

Table 7: Performance of MLE estimators of upper and lower measures of tail dependence, $\Lambda^{(u)}$ and $\Lambda^{(l)}$, obtained by simulating from three different Copulas: a Gumbel with parameter $\theta = 10$, a GH distribution with parameters specified in the second row of Table 1, and a t distribution with parameters $\rho = 0.8$ and $\nu = 3$. Summary measures reported over 1,000 replications for each of two sample sizes are: the mean, standard deviation (std. dev.), and mean squared error (MSE).

References

- [1] AAS, K., AND HAFF, I. H. The Generalized Hyperbolic Skew Student's t -Distribution. *Journal of Financial Econometrics* 4, 2 (2006), 275–309.
- [2] BARNDORFF-NIELSEN, O. Exponentially decreasing distributions for the logarithm of particle size. *Proceedings of The Royal Society A: Mathematical, Physical and Engineering Sciences* 353, 1674 (1977), 401–419.
- [3] BARNDORFF-NIELSEN, O. E. Normal inverse gaussian distributions and stochastic volatility modelling. *Scandinavian Journal of Statistics* 24, 1 (1997), 1–13.
- [4] BIBBY, B. M., AND SØRENSEN, M. Chapter 6 - hyperbolic processes in finance. In *Handbook of Heavy Tailed Distributions in Finance*, S. T. Rachev, Ed., vol. 1 of *Handbooks in Finance*. North-Holland, Amsterdam, 2003, pp. 211 – 248.
- [5] CAMPBELL, R., KOEDIJK, K., AND KOFMAN, P. Increased correlation in bear markets. *Financial Analysts Journal* 58, 1 (2002), 87–94.
- [6] CHERUBINI, U., ELISA LUCIANO, AND VECCHIATO, W. *Market Comovements and Copula Families*. John Wiley & Sons, Ltd, 2004, ch. 3, pp. 95–128.
- [7] CLAYTON, D. A model for association in bivariate life tables and its application in epidemiological studies of familial tendency in chronic disease incidence. *Biometrika* 65:141-151 (1978).

- [8] CM CUADRAS, J. A. A continuous general multivariate distribution and its a continuous general multivariate distribution and its properties. *Comm Statist A - Theory Methods* 10:339-353 (1981).
- [9] COLES, S., HEFFERNAN, J., AND TAWN, J. Dependence measures for extreme value analyses. *Extremes* 2, 4 (Dec 1999), 339–365.
- [10] CUBEROS, A., MASIELLO, E., AND MAUME-DESCHAMPS, V. Copulas checker-type approximations: Application to quantiles estimation of sums of dependent random variables. *Communications in Statistics - Theory and Methods* 49, 12 (2020), 3044–3062.
- [11] EBERLEIN, E., AND PRAUSE, K. The generalized hyperbolic model: Financial derivatives and risk measures. In *MAathematical Finance - Bachelier Congress2000, Geman* (1998), Springer, pp. 245–267.
- [12] EMBRECHTS, P., MCNEIL, A. J., AND STRAUMANN, D. *Correlation and Dependence in Risk Management: Properties and Pitfalls*. Cambridge University Press, 2002, pp. 176–223.
- [13] FERREIRA, M. Nonparametric estimation of the tail-dependence coefficient. *REVSTAT-Stat. J.* 11(1) (2013), 1–16.
- [14] FRANK, M. On the simultaneous associativity of $f(x,y)$ and $x + y - f(x,y)$. *Aequationes Math.*, 19:194-226 (1979).
- [15] FRÉCHET, M. Remarques au sujet de la note précédente. *C R Acad Sci Paris Sér I Math*, 246:2719-2720 (1958).
- [16] FURMAN, E., KUZNETSOV, A., SU, J., AND ZITIKIS, R. Tail dependence of the gaussian copula revisited. *Insurance: Mathematics and Economics* 69 (2016), 97 – 103.
- [17] FURMAN, E., SU, J., AND ZITIKIS, R. Paths and indices of maximal tail dependence. *ASTIN Bulletin* 45, 3 (2015), 661–678.
- [18] GUMBEL, E. Distributions des valeurs extrêmes en plusieurs dimensions. *Publ Inst Statist Univ Paris* 9:171-173 (1960).
- [19] HAMMERSTEIN, E. Tail behaviour and tail dependence of generalized hyperbolic distributions. In *Advanced Modelling in Mathematical Finance*, P. A. Kallsen J., Ed., vol. 189. Springer Proceedings in Mathematics & Statistics, 2016.
- [20] HEFFERNAN, J. E. A directory of coefficients of tail dependence. *Extremes* 3, 3 (Sep 2000), 279–290.
- [21] HILAL, S., POON, S.-H., AND TAWN, J. Hedging the black swan: Conditional heteroskedasticity and tail dependence in s&p500 and vix. *Journal of Banking & Finance* 35, 9 (2011), 2374 – 2387.
- [22] HILL, J. B. On tail index estimation for dependent, heterogeneous data. *Econometric Theory* 26, 5 (2010), 1398–1436.

- [23] HITAJ, A., AND MERCURI, L. Portfolio allocation using multivariate variance gamma models. *Financial Markets and Portfolio Management* 27, 1 (2013), 65–99.
- [24] HOUGAARD, P. A class of multivariate failure time distributions. *Biometrika* 73:671-678 (1986).
- [25] HUA, L., AND JOE, H. Tail order and intermediate tail dependence of multivariate copulas. *Journal of Multivariate Analysis* 102, 10 (2011), 1454 – 1471.
- [26] HUTCHINSON, T., AND LAI, C. Continuous bivariate distributions, emphasising applications. *Rumsby Scientific Publishing, Adelaide* (1990).
- [27] JOE, H. *Multivariate Models and Multivariate Dependence Concepts*. Chapman & Hall/CRC Monographs on Statistics & Applied Probability. Taylor & Francis, 1997.
- [28] LEDFORD, A. W., AND TAWN, J. A. Statistics for near independence in multivariate extreme values. *Biometrika* 83, 1 (03 1996), 169–187.
- [29] LONGIN, F., AND SOLNIK, B. Extreme correlation of international equity markets. *The Journal of Finance* 56, 2 (2001), 649–676.
- [30] MARDIA, K. Families of bivariate distributions. *Griffin, London* (1967).
- [31] MARSHALL, A., AND OLKIN, I. A generalized bivariate exponential distribution. *J Appl Probability* 4:291-302 (1967).
- [32] MARSHALL, A. W., AND OLKIN, I. A multivariate exponential distribution. *J Amer Statist Assoc* 62:30-44 (1967).
- [33] MCNEIL, A. J., FREY, R., AND EMBRECHTS, P. *Quantitative Risk Management: Concepts, Techniques and Tools Revised edition*. No. 10496 in Economics Books. Princeton University Press, October 2015.
- [34] NELSEN, R. B. *An Introduction to Copulas*. Springer Publishing Company, Incorporated, 2010.
- [35] NING, C., AND WIRJANTO, T. S. Extreme return-volume dependence in east-asian stock markets: A copula approach. *Finance Research Letters*, 6 (2009), 202–209.
- [36] POON, S.-H., ROCKINGER, M., AND TAWN, J. Extreme value dependence in financial markets: Diagnostics, models, and financial implications. *The Review of Financial Studies* 17, 2 (2004), 581–610.
- [37] RAMCHAND, L., AND SUSMEL, R. Volatility and cross correlation across major stock markets. *Journal of Empirical Finance* 5, 4 (1998), 397–416.
- [38] ROSSI, E., AND SANTUCCI DE MAGISTRIS, P. Long memory and tail dependence in trading volume and volatility. *Journal of Empirical Finance* 22, C (2013), 94–112.

- [39] SALAZAR, Y., AND NG, W. Nonparametric estimation of general multivariate tail dependence and applications to financial time series. *Statistical Methods & Applications* 24, 1 (March 2015), 121–158.
- [40] SCHLUETER, S., AND FISCHER, M. The weak tail dependence coefficient of the elliptical generalized hyperbolic distribution. *Extremes* 15, 2 (Jun 2012), 159–174.
- [41] SCHMIDT, R. Tail dependence for elliptically contoured distributions. *Mathematical Methods of Operations Research* 55, 2 (2002), 301–327.
- [42] SCHMIDT, R., AND STADTMÜLLER, U. Non-parametric estimation of tail dependence. *Scandinavian Journal of Statistics* 33, 2 (2006), 307–335.
- [43] SEGERS, J., SIBUYA, M., AND TSUKAHARA, H. The empirical beta copula.
- [44] SIBUYA, M. Bivariate extreme statistics, i. *Annals of the Institute of Statistical Mathematics* 11, 3 (Jun 1960), 195–210.
- [45] WANG, J. The multivariate variance gamma process and its applications in multi-asset option pricing. *Dissertation submitted to the Faculty of the Graduate School of the University of Maryland, College Park in partial fulfillment of the requirements for the degree of Doctor of Philosophy* (2009).